Parametrisation and Design of Quadrifilar Helices for use in S-band Satellite Communications

Heather Fraser

A dissertation submitted to the Faculty of Engineering and the Built Environment, University of the Witwatersrand, Johannesburg, in fulfilment of the requirements for the degree of Master of Science in Engineering.

Johannesburg, 2010

Declaration

I declare that this dissertation is my own, unaided work, except where otherwise acknowledged. It is being submitted for the degree of Master of Science in Engineering in the University of the Witwatersrand, Johannesburg. It has not been submitted before for any degree or examination in any other university.

Signed this _____ day of _____ 20___

_____

Heather Fraser

Abstract

This paper is a discussion on the Multiturn Quadrifilar Helix Antenna (QHA) with particular focus on its application as a ground station antenna for S-band communications with a Low Earth Orbit Satellite. A ground station antenna without a tracking system requires a “saddle” shaped, circularly polarised radiation pattern in order to compensate for the change in distance between it and the antenna on the satellite. The Multiturn Quadrifilar Helix can provide this radiation pattern with correct setting of the parameters of pitch, radius and number of turns. The QHA was simulated according to the adjustment of these parameters and the results were assessed. The most suitable results were found for the antennas with low to mid range of number of turns, radii less than 0.22λ and pitch less than 0.6λ. A QHA with 3 turns, pitch of 0.6λ and radius of 0.034λ was suitable for satellite communications. Simulations showed it to have a gain of 6.16dB at 52° and -2.25dB at 0°. Three separate feed networks: a corporate feed network, 90°-180° Hybrid combination and Wilkinson splitter feed network, for the QHA were designed. The antenna was constructed for each feed network and tested. The constructed antennas all had gains less than predicted by simulation. The QHA using the Corporate Feed network had a gain of approximately 10dB less than expected. The QHA using the 90°-180° Hybrid combination feed network had a gain of approximately 8dB less than expected. The best performing QHA was fed by the Wilkinson splitter feed network. It showed good comparison to the shape of the pattern found in simulation but a gain of approximately 6dB lower than expected.

Acknowledgements

I would like to thank the South African Department of Science and Technology for funding this research.

To Professor Alan Clark, thank you for your guidance and for so generously sharing your wisdom and humour.

To my parents; thank you for your support and encouragement.

To my friends at Wits: Mike and Dick for the good company, conversation and help with LaTeX and David for the coffee.

To Craig for always being there to give an ear when I needed to think aloud, to give a hand when I needed to move things I wasn't strong enough to, and to give words of encouragement when I didn't have any of my own. Thank you.

Preface

This dissertation is presented to the University of the Witwatersrand, Johannesburg for the degree of Master of Science in Engineering.

The dissertation is entitled *Parametrisation and Design of Quadrifilar Helices for use in S-band Satellite Communications*

This document complies with the university's *paper model format*. The paper contains the main results and analysis of the research. The appendices present in detail the work conducted during the research.

Contents

List of Figures

List of Tables

Chapter 1

Introduction

1.1 Low Earth Orbit Satellite Communications

Low Earth Orbit (LEO) satellites could be said to be among the most useful type of satellites as they are used for photography, telecomms, scientific and military applications [1]. They orbit at a height of between 180km and 2 000km above the earth's surface [2].

A common antenna used in LEO satellite communication is the narrow beam type [3] often used with a reflector [4]. The antenna is then connected to a sophisticated tracking system which changes its orientation and tracks the satellite. This means that the ground station antenna and the antenna on board the satellite are in constant view of each other for the period of time that the ground station is in the footprint of the satellite as it passes over.

This method requires a large amount of expensive and sometimes complicated equipment to ensure constant view of the satellite antenna [3]. An antenna without such a tracking system would be less expensive and more portable and therefore more desirable [4].

In order to have such a system, a specially designed antenna that would compensate for the lack of tracking system would be required. The most common way of compensating for the tracking device is to design an antenna with an appropriately shaped radiation pattern.

The satellite comes into view of the ground station on the horizon and moves overhead and out of view on the horizon on the opposite hemisphere. As it completes this path the distance from the ground station (and hence the ground station antenna) to the satellite changes with angle. The distance is at its largest when the satellite first comes into view at approximately 60°[5] and at its smallest at $0^{\circ}$when it is directly above the ground station.

Using Friis Link equation [6], Equation 1.1, it can be seen that it is possible to compensate for a change in distance to the antenna on the satellite, r, with a change in gain of the ground station antenna.

$$|S_{21}|^2 = \frac{P_r}{P_t} = \frac{G_r G_t \lambda^2}{(4\pi r)^2} \tag{1.1}$$

$\lvert S_{21}\rvert^2$	= the ratio of power delivered to the receiving antenna to the input power of the transmitting antenna
P_r	= Power received
P_t	= Power Transmitted
G_r	= Gain of receiving antenna
G_t	= Gain of transmitting antenna
λ	= Wavelength in metres
r	= Distance between antennas

This equation can be adapted to include the mismatch between cables and antennas as follows [6]:

$$|S_{21corrected}| = |S_{21}|\, M_{11} M_{22} \tag{1.2}$$

Where:

$$M_{11} = 1 - \left(\frac{\frac{1+S_{11}}{1-S_{11}} - 1}{\frac{1-S_{11}}{1+S_{11}} + 1} \right)^2 \tag{1.3}$$

and

$$M_{22} = 1 - \left(\frac{\frac{1+S_{22}}{1-S_{22}} - 1}{\frac{1-S_{22}}{1+S_{22}} + 1} \right)^2 \tag{1.4}$$

Where:

$|S_{21}|$: the ratio of power delivered to the receiving antenna to the input power of the transmitting antenna
M_{11} : Compensation coefficient of antenna 1
M_{22} : Compensation coefficient of antenna 2
S_{11} : Reflection coefficient of antenna 1
S_{22} : Reflection coefficient of antenna 2

A more constant S_{21} can be created by having a radiation pattern with gain that changes according to angle. When the distance, r, is larger the gain must be larger to compensate for the greater r in Equation 1.1. Conversely when the distance, r, is smaller the gain of the antenna must be smaller. Therefore a "saddle shaped" radiation pattern with higher gain at $\pm 60^\circ$, when the satellite first comes into view of the groundstation but is further away, than at the centre, when it is closer, is required [5].

The antenna must also be circularly polarised. This is due to the fact that the satellite orientation may be different on each pass over the base station and to align the antennas exactly would cost time that could be used for communication with the satellite [7].

1.2 Proposed Solution

A number of suitable antennas exist to provide the desired saddle shaped radiation pattern. The bifilar helix can provide the required saddle shaped radiation pattern but has high backlobe levels [8]. A triangular patch antenna array has also been shown to produce the required shape [9] but the most common and appropriate of the researched antennas appeared to be the multiturn backfire quadrifilar helix [5].

The multiturn quadrifilar helix antenna is an extension of the quadrifilar helix antenna described by Kilgus in 1970 [10]. It had previously been discussed by Gerst and Worden in 1964 [11]. The QHA consists of four helices equally spaced on a cylinder and fed 90°out of phase (ie one helix is fed at 0°, one at 90°, one at 180°and one at 270°) [12]. These helices are shorted together at the top of the antenna. This is sometimes described as being two, bifilar helices fed 180°out of phase [13] The antenna can be used with [12] or without [5] a ground plane. In a standard QHA the number of turns of the helix N=1. N can also be a fraction as in the fractional turn QHA [13] or an integral number as in the multiturn QHA. [5].

The QHA can be described using a set of parameters as follows.

r_0 radius
P pitch distance for one element measured along the axis of the helix
N Number of Turns of the helix

As an illustration the drawing by Kilgus, [5] can be seen in *Figure 1.1*

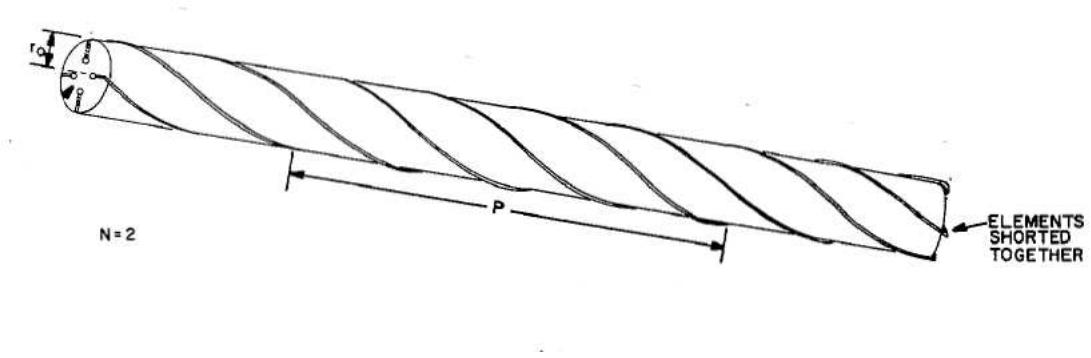

Figure 1.1: Quadrifilar Helix Antenna [5]

Walter Maxwell described the $\frac{\lambda}{2}$ QHA as "evolving" from a pair $\frac{\lambda}{2}$ square loop antennas [14]. The loop has sides of $\frac{\lambda}{4}$ long and the current flows 'in' one side of the loop and 'out' the other. Now if this loop is twisted around a cylinder (of desired radius) it becomes a bifilar helix. Two of these twisted loops placed orthogonally and fed 180°out of phase create a $\frac{\lambda}{2}$ quadrifilar helix antenna [14].

In his 1974 paper [5] Kilgus described the effects of changing these parameters. His paper describes QHAs with 1-5 turns, pitches of 0 to 1 λ and radii of 0.01 to 0.14 λ. He noted that there was a region of shaped-conical beams between Pitch = 0.3λ and 0.9λ and Radius = 0.01λ and 0.14λ. The shapes of these beams do however vary and while Kilgus noted the most useful of these [5] he did not list a full set of results. The antennas are described in terms of the parameter k which is the ratio of radius, r_0, to pitch, p.

He noted that an antenna for the purpose of satellite communications occurs when $k = 0.083$ and $p = 0.6$ with N=3, $k = 0.083$ and $p = 0.609$ when N = 5. A full description of these regions is not, however, presented.

A more detailed description of the variation of performance of the multiturn QHA with number of turns, pitch and radius would be very useful when deciding on the parameters of the QHA for a specific purpose.

Using simulation software it is now possible to do many simulations for a variety of parameter changes. The research presented in this paper details the performance of the QHA for a wider variation of parameters. Using the simulation package SuperNEC, [15], a series of QHAs were simulated. Widening the range that Kilgus used these antennas had pitches ranging from 0.1λ to 0.9λ in steps of 0.1λ, radii from 0.01λ to 0.3λ in steps of 0.01λ. The simulations were performed for antennas with an integral number of turns ranging from 1 to 8 turns. The full set of results can be found in Appendix D [16]. An antenna suitable for satellite communications was then constructed and tested and the design of the feed network for this antenna together with the results of tests are presented.

References

[1] Peter Berlin. *Satellite Platform Design*. Kiruna Space and Environment Campus, 2003.

[2] NASA. Catelog of Earth Satellite Orbits. www.earthobservatory.nasa.gov/Features/OrbitsCatalog. Last accessed 28 November 2009.

[3] Ali Mirkamali, Lida Akhoondzadeh, Kiyan Keyghobad, and Mohammad Soleimani. A Novel Quadrifilar Helix Antenna For Use in LEO Satellite Communications. *International Conference on Antenna Theory and Techniques*, pages 509–511, September 2003.

[4] Stephen D. Targonski. A Multiband Antenna for Satellite Communications on the Move. *IEEE Transactions on Antennas and Propagation*, 54(10):2862–2868, October 2006.

[5] Charles C. Kilgus. Shaped-Conical Radiation Pattern Performance of the Backfire Quadrifilar Helix. *IEEE Transactions on Antennas and Propogation*, May:392–397, 1975.

[6] A Rudge, K Milne, A Oliver, and P Knight. *The Handbook of Antenna Design*, volume 1. Peter Peregrinus, Ltd, 1982.

[7] Personal Communication. Keith Palmer. University of Stellenbosch, October 2008.

[8] K. M. Keen, D. Smith, and B. S. Lee. Improved Form of Backfire Bifilar Helix Conical Beam Antenna. *Microwave and Optical Technology Letters*, 14(5):278–280, April 1997.

[9] Josaphat Tetuko Sri Sumantyo, Koichi Ito, and Masaharu Takahashi. Dual-Band Circularly Polarized Equilateral Triangular-Patch Array Antenna for Mobile Satellite Communications. *IEEE Transactions on Antennas and Propagation*, 53(11):278–280, November 2005.

[10] Charles C. Kilgus. Resonant Quadrifilar Helix Design. *Microwave Journal*, 13:49–54, 1970.

[11] C. Gerst and R. A. Worden. Helix Antennas Take Turn for the Better. *Electronics*, August:100–110, 1966.

[12] Arlon T. Adams, Robert K. Greenough, Robert F. Wallenberg, Ada Mendelovicz, and C. Lumjiak. The Quadrifilar Helix Antenna. *IEEE Transactions on Antennas and Propogation*, AP-22(2):100–110, March 1974.

[13] Charles C. Kilgus. Multielement, Fractional Turn Helices. *IEEE Transactions on Antennas and Propagation*, pages 499–500, July 1968.

[14] Walter Maxwell. Quadrifilar Helix Antenna-Part of the Reflections 2 Series. http://w2du.com/r2ch22.pdf. Last accessed 28 November 2009.

[15] Poynting Innovations. SuperNEC. www.supernec.com. Last accessed 30 November 2009.

[16] Heather Fraser. Appendix D - Simulations and Results. M.Sc, University of the Witwatersrand, 2009.

Part 1

Paper: Parametrisation and Design of Quadrifilar Helices for Use in S-band Satellite Communications

Parametrisation and Design of Quadrifilar Helices for use in S-band Satellite Communications

Heather Fraser

***Abstract*—This paper is a discussion on the Multiturn Quadrifilar Helix Antenna (QHA) with particular focus on its application as a ground station antenna for S-band communications with a Low Earth Orbit Satellite. A ground station antenna without a tracking system requires a "saddle" shaped, circularly polarised radiation pattern in order to compensate for the change in distance between it and the antenna on the satellite. The Multiturn Quadrifilar Helix can provide this radiation pattern with correct setting of the parameters of pitch, radius and number of turns. The QHA was simulated according to the adjustment of these parameters and the results were assessed. The most suitable results were found for the antennas with low to mid range of number of turns, radii less than 0.22λ and pitch less than 0.6λ. A QHA with 3 turns, pitch of 0.6λ and radius of 0.034λ was suitable for satellite communications. Simulations showed it to have a gain of 6.16dB at 52° and -2.25dB at 0°. Three separate feed networks: a corporate feed network, 90°-180° Hybrid combination and Wilkinson splitter feed network, for the QHA were designed. The antenna was constructed for each feed network and tested. The constructed antennas all had gains less than predicted by simulation. The QHA using the Corporate Feed network had a gain of approximately 10dB less than expected. The QHA using the 90°-180° Hybrid combination feed network had a gain of approximately 8dB less than expected. The best performing QHA was fed by the Wilkinson splitter feed network. It showed good comparison to the shape of the pattern found in simulation but a gain of approximately 6dB lower than expected.**

***Index Terms*—Satellite Antennas, Quadrifilar Helix Antenna, Phase shifting/splitting networks**

I. Introduction

The primary requirement of this research was to find a cheap, mobile antenna for use in satellite communications. The antenna designed was required to have a cardiod shaped radiation pattern to compensate for the change in distance to a satellite as it passed over a base station. A suitable antenna to fit this requirement is a Quadrifilar Helix Antenna [1]. The radiation pattern of this antenna can be varied by adjusting the pitch, radius and number of turns of the antenna.

Research into these antennas has been conducted by others, most notably Charles Kilgus. Kilgus's research was, however, conducted in the 1960's when computer aided simulation was not widely available as a design tool. Therefore only a limited number of parameter variations of the antenna were explored as the results were found by time-consuming construction and testing. Modern processors and simulation packages now make it possible to simulate thousands of variations of an antenna and view the effect on its performance. The antenna designed was found from a series of simulations varying the parameters of the QHA. The results of all simulations are presented in [2] and were arranged according to possible uses.

II. Background Information

A Low Earth Orbit (LEO) satellite orbits the earth at between 180km and 2 000km above its surface[3]. LEO satellites are very useful satellites and are used for photography, telecommunications and scientific as well as military applications [4]. The ground station antenna used to communicate with a low earth orbit satellite is often of the narrow beam type with a tracking system [5]. This antenna then tracks the satellite and constant communication is kept. This method is, however, bulky and expensive.

As an alternative a simpler antenna can be used. This antenna must have a shaped cardiod radiation pattern which has a gain at 0° of approximately 10 dBs less than at 60° [1]. This is in order to compensate for the change in distance to the satellite as it passes over the ground station. The antenna must also be circularly polarised so that any misalignment of the antennas due to the rotation of the satellite antenna on its own axis does not cause problems [6]. The antenna designed was desired for use at S-band frequencies. The particular frequency of interest was 2.245 GHz.

III. Discussion of Researched Methods

A. Antennas

Literature suggested [5], [7] that the use of a Quadrifilar Helix Antenna (QHA) would be most suitable for the creation of a shaped radiation pattern as described. This antenna described by Kilgus [1] consists of four helices fed in phase quadrature. It is capable of radiating a cardiod shaped, circularly polarised pattern [1].

There are a number of different "varieties" of QHA including the multi-turn backfire, self-resonant and fractional-turn QHA. Fractional turn helices are used on board satellites due to their cardiod shaped and circularly polarised radiation patterns [8] Kilgus demonstrated in his 1975 paper that the backfire helix which he realised by extending the multi-turn QHA to an integral number of turns showed excellent circular polarisation as well as a shaped beam whose shape could be adjusted by setting the parameters of the QHA. Any of the QHAs can either be shorted at the top [1] of the antenna or left open [9].

B. Feed Networks

The QHA requires each arm to be fed 90° out of phase with that before it. In order to achieve this a phasing feed network is required. This network must have four outputs of equal magnitude and phase 90°, 180°, 270° and 360°.

There are a number of ways of achieving this. All methods investigated involved couplers created using microstrip line. A branchline coupler [10] produces two equal magnitude outputs 90° out of phase and could be used in combination with a 180° or "rat-race" hybrid which produces two equal magnitude outputs 180° out of phase [11] to produce the desired phase shifted outputs.

A corporate feed network [12] or Wilkinson splitter [11] could be used to split the signal into four equal parts and a series of

meandering lines could then be used to set the phase differences going to each branch.

IV. DESCRIPTION OF CHOSEN METHODS

A. Antenna

Kilgus showed that the backfire quadrifilar helix antenna has a radiation pattern that is significantly varied according to its physical parameters [1]. Among these variations is a cardiod shape that may be suitable for LEO satellite communications. For this reason an adaption of the backfire quadrifilar helix antenna was chosen for simulation and design. The original backfire QHA described by Kilgus was fed at the top of the antenna [1]. The antenna simulated and designed for this research was fed at the bottom of the antenna; thereby removing the "backfire" element. As in Kilgus's research the antenna was simulated for an integral number of turns.

The QHA can be described according to a number of parameters:

- **Number of turns:** The number of revolutions each helix of the QHA makes.
- **Pitch:** The distance between the same point on consecutive turns of one element.
- **Radius:** The radius of the circular area enclosed by the QHA.

Figure 1 shows a diagram of the antenna [1].

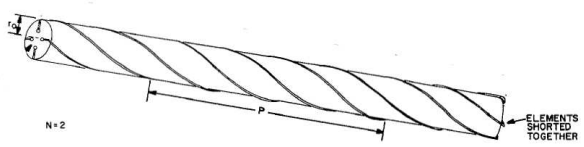

Fig. 1: Quadrifilar Helix Antenna [1]

The radiation pattern varies with the adjustment of the above parameters. For this reason a series of simulations were performed to establish how each parameter affects the radiation pattern. From this information an antenna suitable for satellite communications could be found and constructed.

B. Feed Networks

1) Branchline Coupler and 180° Hybrid: The branchline coupler (90° hybrid), *Figure 2*, is a quadrature coupler [10]. This means that it has one input which is split into two, equal magnitude outputs that are 90° out of phase. This on its own is not however sufficient to create the four inputs necessary. It consists of a square with sides equal to $\frac{\lambda}{4}$ or a circle of circumference 1λ. The parallel sections have a characteristic impedance of $\frac{Z_0}{\sqrt{2}}$ and the series sections have a characteristic impedance of Z_0 [11]. If two branchline couplers are used then the outputs will each be 90° apart if their inputs are 180° out of phase.

In order to create these inputs a 180° or rat-race hybrid, *Figure 3*, can be used. This is a four arm device with the phase of the outputs depending on which input is used. It consists of a ring of circumference 1.5λ and Z_0 of $\sqrt{2}Z_0$ with four arms, each of characteristic impedance Z_0, spaced $\frac{\lambda}{4}$ apart.

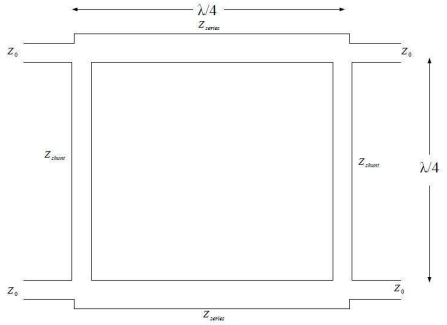

Fig. 2: Branchline Coupler

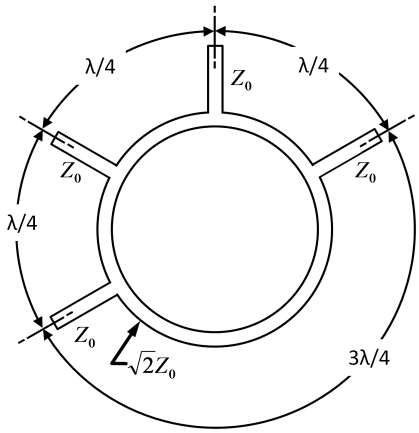

Fig. 3: 180° Hybrid

2) Corporate Feed with Meandering Lines: The corporate feed network does not work on the same principle of coupling as the above solutions. It uses the principle of matching sections of transmission line to split the signal [12] . A section of 50Ω transmission line is split into four sections of 75Ω transmission line. Each of these lines is $\frac{\lambda}{4}$ long in order to act as an impedance matcher [12]. A set of meandering lines must be used for phasing in order to achieve the required phase difference.

3) Wilkinson Splitter: The Wilkinson Splitter was designed by E. Wilkinson. It can be used to split a signal into equal magnitude and equal phase portions. An N-way splitter is simple to design but requires cross over pieces and so is more difficult to manufacture. Therefore three, 2-way splitters could be used. Each Wilkinson splitter, *Figure 4*, consists of a section of transmission line of characteristic impedance, Z_0. This then splits into two sections with impedance $\sqrt{2}Z_0$ and $\frac{\lambda}{4}$ long. A section of transmission line of characteristic impedance Z_0 is connected to each of these sections. At the point of connection an isolation resistor of value $2Z_0$ is connected between the two transmission lines.

V. SIMULATION PROCEDURE

The QHA was simulated in the Method of Moments simulation package, SuperNEC [13]. A "test" set of simulations was performed. In these simulations a selection of the antennas described by Kilgus in [1] were simulated. The results were directly comparable to those presented by Kilgus and so the next set of simulations was performed.

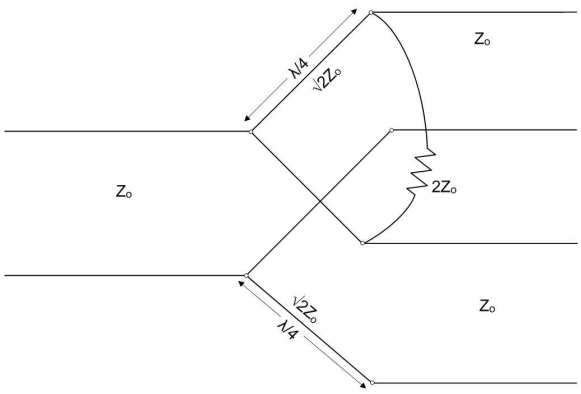

Fig. 4: N=2 Wilkinson Splitter

Kilgus showed that useful results for the Backfire Quadrifilar Helix were found for pitches of 0.3λ to 0.85λ and radii of 0.01λ to 0.13λ [1]. Seven sets of simulations were performed with the number of turns of the QHA increasing incrementally from 2 to 8. This was in order to extend slightly beyond the borders of the range of simulations performed by Kilgus and observe as many useful results as possible. Each of these antennas was simulated with pitches ranging from 0.1λ to 0.9λ in steps of 0.1λ and radius from 0.01λ to 0.3λ in steps of 0.01λ. These ranges also extend slightly beyond the range used by Kilgus. Due to the large number of simulations performed an ideal ground plane was used in order to reduce simulation time. A comparison of a simulation with an ideal ground plane with that of a square ground plane of length $\frac{\lambda}{2}$ was made in order to establish that this approach was valid. The results were comparable and so the use of an ideal ground plane was valid.

VI. RESULTS

Over the range of simulations a number of trends were noted. Each of the parameters adjusted in the simulations had an effect on the performance of the antenna; particularly the shape, and hence usefulness, of the radiation pattern.

A. Number of Turns

The number of turns of the QHA greatly affected its performance. In general the QHAs with the lower number of turns showed better radiation patterns. This is to say that these radiation patterns had less ripple and better VSWR than those with more turns. This can be seen in *Figure 5* and *Figure 6*. Looking at the radiation pattern alone there were 24 antennas found, for N=2 turns, that had a radiation pattern suitable for satellite communications. For N=8 turns, however, only 4 antennas with suitable radiation patterns were noted.

B. Pitch

The QHAs with a lower pitch, generally less than 0.6λ-0.7λ had good general performance. This is to say that they had a smooth beam but not the cardiod shape desired. This shape was more commonly found in QHAs with mid range pitches. All the QHAs with pitches higher than 0.7λ had very rippled or distorted radiation patterns that would not be suitable for any applications.

C. Radius

At a set pitch the performance of the antenna varied with radius. The QHAs with lower pitch had good "general" performance for all radii but not anything suitable for satellite communications as required. In QHAs with mid range pitches the lower radii produced more cardiod shaped patterns. The VSWR of the QHA improved as the radius increased.

D. General Regions

When the results were grouped, according to the number of turns of each QHA and the type of result plotted as a function of radius and pitch, three distinct regions could be seen. The results for N=2 turns, *Figure 5*, illustrates this point. The dots mark antennas showing a radiation pattern with a shaped radiation with gain increasing from a minimum at 0° and therefore possibly useful for satellite communications. The crosses represent antennas which showed a smooth and undistorted radiation pattern which may be used for other, more general, uses. The antennas with rippled or distorted patterns are not shown on this graph. A line separating the region in which they occur and the area in which useful patterns were found can be drawn. For the QHA with N=2 this line has the equation $P = -1R + 0.66$ where P is the pitch of the antenna and R is the radius.

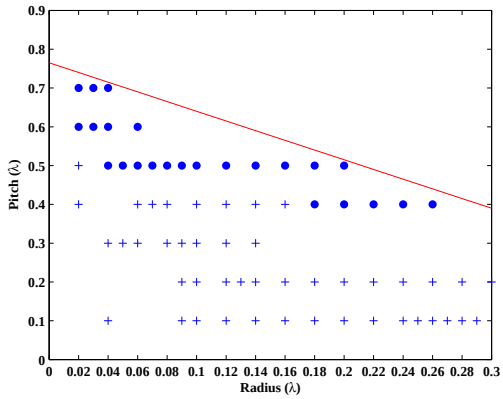

Fig. 5: Results for N=2 turns showing antennas suitable for general use (+) and those suitable for use in satellite communication(●)

As can be seen in *Figure 5* the "usefulness" of the antenna falls into three distinct regions according to the classifications described. There is a very distinct line between the areas of usefulness and the region where the radiation pattern is too rippled or distorted for use. This line changed with the number of turns of the antenna. By way of example see *Figure 6* which shows a similar graph for the QHA with 8 turns. As can be seen in this graph there are fewer useful antennas, both for satellite and general use. The area of the graph where the rippled and distorted patterns fall is much larger than for 2 turns. The line separating the regions can also be seen to be steeper with a lower intercept on the y-axis. This shows that as the number of turns of the QHA increases the number of useful antennas achievable decreases. This is possibly due to the fact that as the number of turns increases the amount of capacitance increases (due to the larger number of parallel sections) having a negative effect on the radiation pattern.

E. Most Suitable QHA for Satellite Communications

The most suitable radiation patterns that fit the requirements outlined for satellite communications were found for a QHA with

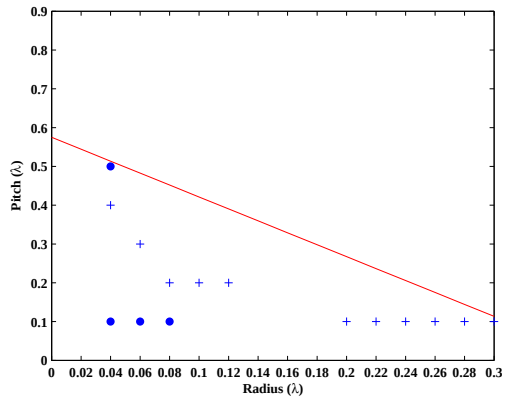

Fig. 6: Results for N=8 Turns

3 turns, a pitch of 0.6λ and a radius of approximately 0.03λ. Further simulations with finer iterations were performed in this region and the results can be seen in Table 1.

Table 1: Further simulations for N=3 Turns and Pitch=0.6λ

Radius(λ)	Centre Gain(dB)	Edge Gain(dB)	VSWR
0.031	-1.85	6.18	1.54
0.032	-2.0	6.18	1.36
0.033	-2.1	6.17	1.21
0.034	-2.25	6.16	1.07
0.035	-2.4	6.11	1.10
0.036	-2.51	6.10	1.23
0.037	-2.61	6.08	1.37
0.038	-2.67	6.06	1.52
0.039	-2.74	6.05	1.69

Out of the above results the antenna with the best VSWR was chosen for construction. This was the QHA with a pitch of 0.6λ and radius of 0.034λ. The radiation pattern can be seen in *Figure 7*. As can be seen in the figure and in Table 1 this pattern has a maximum gain of 6.16dB. This occurs at approximately 52°. The gain at 0° is -2.25dB. This is a difference of 8.41dB over the 52° and is very suitable for the application of satellite communications[1]

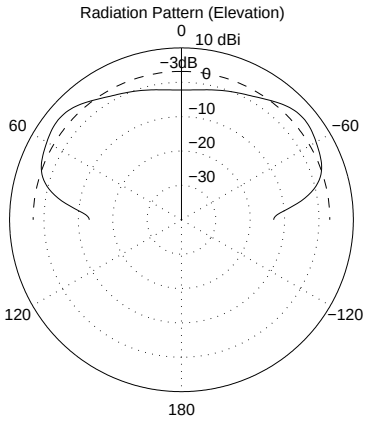

Fig. 7: Radiation pattern of constructed QHA

VII. CONSTRUCTING THE ANTENNA

A. Antenna

The QHA was constructed by hand and no special tooling or machinery was used. The following process was followed.

The antenna "pattern" was marked out on cardboard. The card board was cut to be as wide as the circumference of the antenna. It was then divided into four equal sections vertically. Horizontal lines spaced 80mm (0.6λ at 2.245GHz) apart were then drawn. The intersections of these wires were colour coded to follow a spiral pattern. ie. a red intersection would be followed by a blue, then a green and finally a black. The sequence was then repeated. The piece of cardboard was then wrapped around a dowel of radius 8mm.

Four lengths of copper wire, of width = 1mm so that the antenna would be stiff enough to support itself, were then wound around the dowel; each following a colour sequence. By following this process four spirals of equal angle and pitch were created. The four wires were then soldered together at the top of the dowel. The arrangement was held in place for two days in order to let the wire take shape.

The cardboard together with the QHA were removed from the dowel. The free ends of the wire were then soldered onto which ever feed network was desired. *Figure 8* shows the constructed antenna.

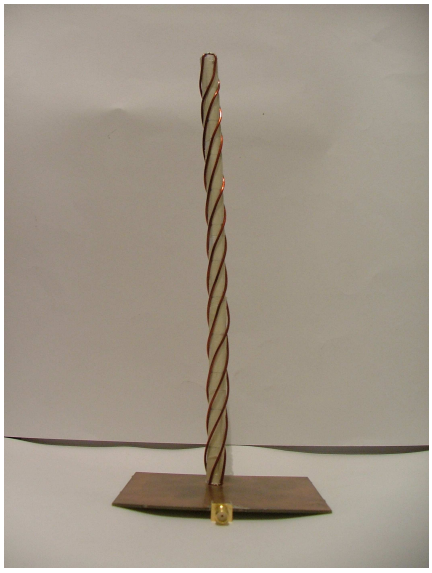

Fig. 8: Constructed QHA

B. Feed Network

1) Design: The feed networks were designed for construction from microstrip line on a board of FR-4. Each feed network required sections of transmission with specific characteristic impedances. A specific characteristic impedance can be achieved on microstrip line by setting the width to height ratio of the microstrip line [10].

This is done using a set of equations described by Gardiol [12] which are set for two cases: when the width to height ratio of the microstrip line is less than 1 and when it is greater than or equal to 1.

For w/h $<$ 1

$$\epsilon_{eff} = \frac{\epsilon_r + 1}{2} + \frac{\epsilon_r - 1}{2}\left(\frac{1}{\sqrt{1+\frac{12}{w/h}}} + 0.04(1-w/h)^2\right) \quad (5)$$

and

$$Z_0 = \frac{60}{\sqrt{\epsilon_{eff}}} \ln\left(\frac{8}{w/h + \frac{w/h}{4}}\right) \quad (6)$$

For the case where w/h ≥ 1

$$\epsilon_{eff} = \frac{\epsilon_r + 1}{2} + \frac{\epsilon_r - 1}{2}\left(\frac{1}{\sqrt{1 + \frac{12}{w/h}}}\right) \quad (7)$$

and

$$Z_0 = \frac{120\pi}{\sqrt{\epsilon_{eff}}} \div (w/h + 1.393 + 0.667 \ln(w/h + 1.444)) \quad (8)$$

These equations were adjusted as described in [14] to find the desired Z_0 for each section of transmission line. The permittivity of the FR-4 was assumed to be 4.4 for the 90°-180° hybrid combination and corporate feed networks. When these were tested the value of Z_0 was not as expected. Further tests were done and these tests showed that the value of permittivity used was incorrect [14] and it was changed to 5.4 for the Wilkinson splitter.

Using the above equations the parameters of each network were as follows:

180° - 90° Hybrid: The parameters of the Branchline Coupler-Hybrid Ring feed network can be seen in Table 2.

Table 2: Branchline Coupler Hybrid Ring Combination Network

Description	Electrical Length	Physical Width(mm)	Physical Length(mm)
90° hybrid: 50Ω sections	$\frac{\lambda}{4}$	3.06	18.3
90° hybrid: 35.4Ω sections	$\frac{\lambda}{4}$	5.2	17.9
180° hybrid 70.7Ω ring	1.5λ	1.606	112.5

Corporate Feed: The properties of the Corporate Feed network can be seen in Table 3.

Table 3: Corporate Feed Network

Description	Electrical Length	Physical Width(mm)	Physical Length(mm)
75Ω sections	$\frac{\lambda}{4}$	1.42	18.83
90° phasing	$\frac{\lambda}{4}$	3.06	18.3
180° phasing	$\frac{\lambda}{2}$	3.06	36.6
270° phasing	$\frac{3\lambda}{4}$	3.06	54.9
360° phasing	1λ	3.06	73.2

Wilkinson splitter: The Wilkinson Splitter was designed after more tests had been performed on the FR-4 to get a more accurate description of its permittivity. The iterative process of satisfying Equations B.1- B.4 was repeated and the properties of the Wilkinson Splitter network were as in Table 4.

2) Construction: The feed networks were drawn in the circuit layout program EAGLE and milled out on a circuit milling machine at the University of the Witwatersrand. Three QHAs were constructed and soldered onto each feed network and tested. *Figure 9* shows the 90°-180° Hybrid combination feed network, *Figure 10* shows the Corporate Feed network and *Figure 11* shows the Wilkinson splitter feed network. An SMA connector was soldered onto each of the feed networks to enable connection to a cable.

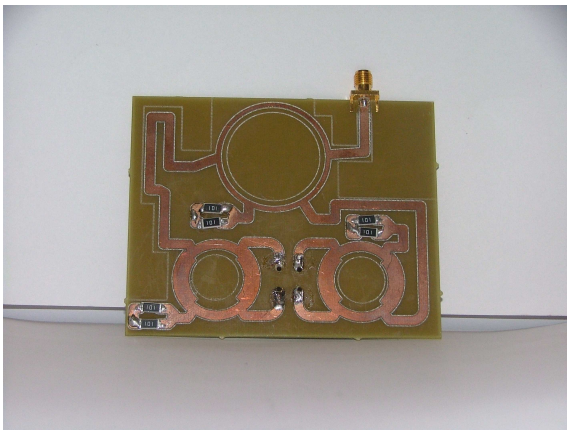

Fig. 9: 180° and 90° hybrid combination

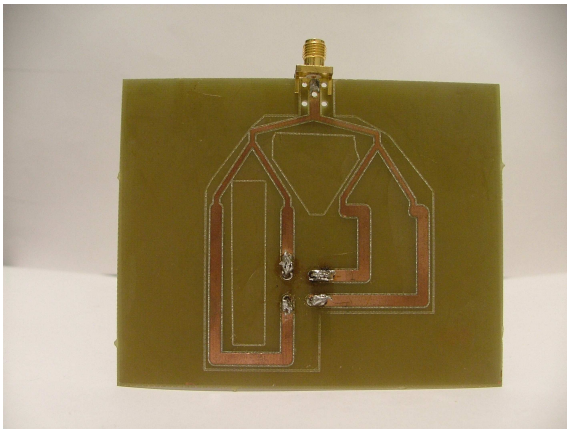

Fig. 10: Corporate Feed

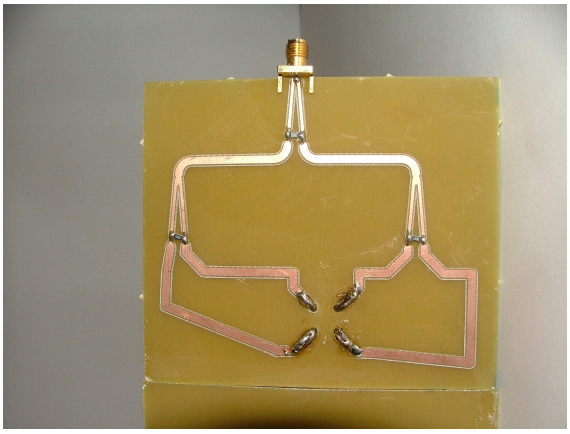

Fig. 11: Wilkinson Splitter

Table 4: Wilkinson Splitter

Description	Electrical Length	Physical Width(mm)	Physical Length(mm)
$\sqrt{2}Z_0$ sections	$\frac{\lambda}{4}$	1.33	17.22
90° phasing	$\frac{\lambda}{4}$	2.62	16.78
180° phasing	$\frac{\lambda}{2}$	2.62	33.56
270° phasing	$\frac{3\lambda}{4}$	2.62	50.35
360° phasing	1λ	2.62	67.13

VIII. TESTING AND RESULTS

The three QHAs with feed networks were tested in the anechoic chamber at the University of the Witwatersrand. An LPDA antenna was used as the transmit antenna and the QHA as the receive antenna. The QHA was rotated in 5° increments and a HP8753C network analyser was used to take measurements of S_{21} which were converted to Gain and plotted.

A. QHA with 90° and 180° Hybrid Combination Feed Network

The plot of the radiation pattern of the QHA with the 90°-180° feed network combination can be seen in *Figure 12*. In its polar form the radiation pattern does not look close to what was expected but a linear plot shows the performance much better. There is a definite decrease in gain towards 0° and a peak at approximately 60°.

The gain of this arrangement is, however, approximately 8dB lower than that expected from simulation results.

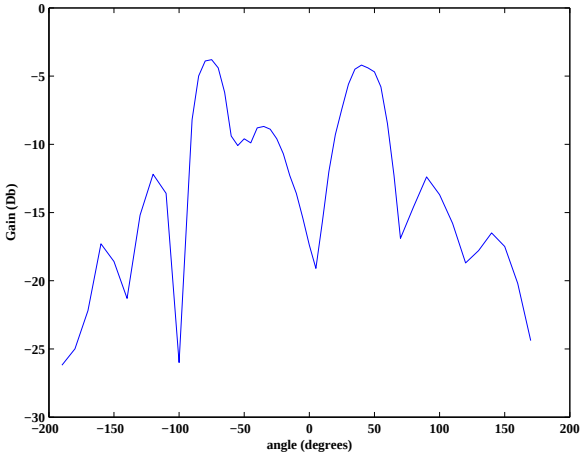

Fig. 12: Radiation Pattern of 90°-180° hybrid combination

B. QHA with Corporate Feed

The plot of the radiation pattern of the QHA with the Corporate Feed network can be seen *Figure 13*. The linear version is again presented due to the poor visibility of the pattern in polar format. As can be seen there is a decrease in gain towards 0°. This arrangement, however, shows noticeable side lobes. The gain is, as for the 90°-180° combination feed much lower (approximately 10dB) than expected.

C. QHA with Wilkinson Splitter Feed

This arrangement proved the best performing of the three combinations. As can be seen in *Figure 14* the radiation pattern shape agrees very well with the shape predicted by the simulation. The maximum is at approximately ±55° and the minimum is at 0°. The gain is still lower than predicted but significantly better than the previously discussed feed networks by approximately 3 to 4 dB.

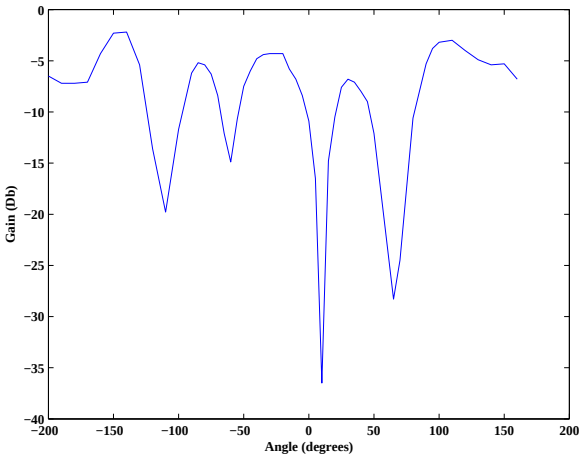

Fig. 13: Radiation Pattern of Corporate Feed Fed QHA.

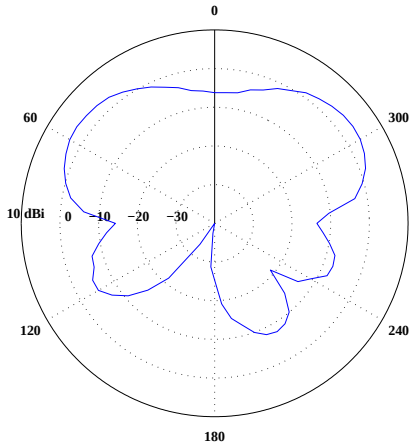

Fig. 14: Radiation Pattern of Wilkinson Splitter fed QHA

IX. DISCUSSION OF RESULTS

The gain of the radiation patterns is significantly lower than that expected. This could be due to a number of reasons:

Coupling: As can be seen in *Figure 10* and *Figure 9* the tracks of both the Corporate Feed network QHA and the 90°-180° feed network are, in parts, close together. This may cause coupling between the tracks and, hence, losses on the network producing a lower gain due to lower input than the tests showed.

Incorrect Z_0: As a result of the poor performance of the QHAs with Corporate Feed and 90°-180° feed networks a series of tests were performed on the FR-4 board used to construct the feed networks in order to more accurately determine the permittivity of

the board. These included short circuit, open circuit and load tests and are detailed in [14]. The permittivity found was higher than that initially used. This value was used when designing the Wilkinson power divider. It is possibly for this reason that the QHA with Wilkinson power divider feed network had a higher gain than the other feed networks.

Poor Construction: As each QHA was constructed by hand without any specialised tooling the parameters of the QHA (pitch, radius) may not have been as accurate as required. At the frequency of design, 2.245GHz, one wavelength is only 0.1336m. This means that 0.1λ would correspond to 13mm. As can be seen in the results presented in [2] and [15] a 0.1λ difference in either pitch or radius could have a significant effect on the performance of the QHA. A 13mm shift in pitch or radius would therefore have an effect on the performance of the antenna.

Isolation Between Output Ports: The shape of the radiation patterns shows a trend similar to that found from simulation. The corporate feed network is the poorest performing of all the feed networks. This network has little to no isolation between output ports. The 90°-180° feed network combination has a larger degree of isolation between output ports and its performance is slightly better. The most accurately performing of the three feed networks is the Wilkinson splitter arrangement. This is possibly due to the fact that the output ports of this network are more isolated from each other than the other arrangements [16]. This isolation is due to the resistors between the output ports shown in *Figure 11.*

Cardboard: The cardboard support for the antenna was left in place when the three antennas were tested. To view its effect on the radiation pattern it was removed for one set of tests using the best performing of the three feed networks, the Wilkinson splitter arrangement. A significant effect was noted with the gain of the antenna increasing by approximately 3.4dBs. There was no effect on the shape. For this reason a study into the effect of a dielectric support for the QHA should be conducted.

X. CONCLUSION

The multiturn Quadrifilar Helix antenna was simulated and the most suitable antenna for S-band satellite communications was constructed and tested. The results agreed well with simulation with regard to shape but agreed poorly with regard to gain.

REFERENCES

[1] Charles C. Kilgus. Shaped-Conical Radiation Pattern Performance of the Backfire Quadrifilar Helix. *IEEE Transactions on Antennas and Propogation*, May:392–397, 1975.

[2] Heather Fraser. Appendix D - Simulations and Results. M.Sc, University of the Witwatersrand, 2009.

[3] NASA. Catalog of earth satellite orbits. www.earthobservatory.nasa.gov/Features/OrbitsCatalog. Last accessed 28 November 2009.

[4] Peter Berlin. *Satellite Platform Design*. Kiruna Space and Environment Campus, 2003.

[5] Ali Mirkamali, Lida Akhoondzadeh, Kiyan Keyghobad, and Mohammad Soleimani. A Novel Quadrifilar Helix Antenna For Use in LEO Satellite Communications. *International Conference on Antenna Theory and Techniques*, pages 509–511, September 2003.

[6] Personal Communication. Keith Palmer. University of Stellenbosch, February 2007.

[7] R. Cahill, I. Cartmell, G van Dooren, K Clibbon, and C Sillence. Performance of Shaped Beam Quadrifilar Antenna on the Metop Spacecraft. *IEE Procedings on Microwaves, Antennas and Propogation*, 145(1):19–24, February 1998.

[8] Muhammed Amin and Robert Cahill. Resonant Quadrifilar Helix Design. *IEEE Microwave and Wireless Components Letters*, 16(6):384–386, June 2006.

[9] Walter Maxwell. Quadrifilar Helix Antenna-Part of the Reflections 2 Series. http://w2du.com/r2ch22.pdf. Last accessed 28 November 2009.

[10] David M Pozar. *Microwave Engineering*. John Wiley and Sons, Inc, 1998.

[11] Harlan Howe Jr. *Stripline Circuit Design*. Artech House, 1985.

[12] Personal Communication. Prof Alan Clark. University of the Witwatersrand, May 2008.

[13] Poynting Innovations. SuperNEC. www.supernec.com. Last accessed 30 November 2009.

[14] Heather Fraser. Appendix B - Design of Feed Network for a Quadrifilar Helix Antenna. M.Sc, University of the Witwatersrand, 2009.

[15] Heather Fraser. Appendix A - Analysis of Simulations. M.Sc, University of the Witwatersrand, 2009.

[16] Personal Communication. Derek Nitch. Poynting Antennas, November 2008.

Part 2

Appendices

Appendix A

Analysis of Simulations

A.1 Introduction

In order to observe a significant number of radiation pattern variations in the multiturn quadrifilar approximately 2000 simulations of the antenna were performed. This document presents a summary of the radiation patterns observed according to the antenna parameters.

A.2 Description of the Simulation Process

A.2.1 SuperNEC

SuperNEC is a method of moments simulation package developed by Poynting Innovations. It uses a method of moments software to solve electromagnetic problems [1]. The package has a pre-defined quadrifilar helix antenna structure for use in simulations. This is the structure that was used in simulations and an example of it can be seen in *Figure A.1*.

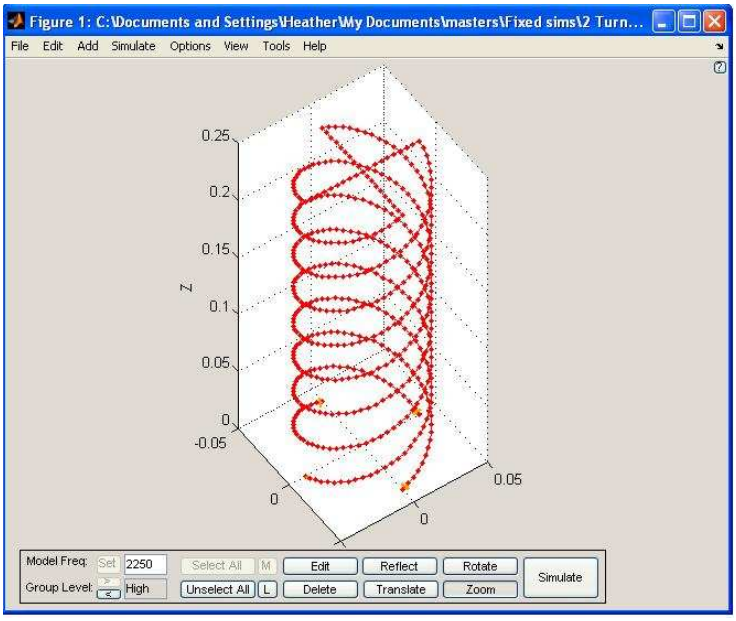

Figure A.1: Quadrifilar Helix antenna as seen in SuperNEC simulation environment

A.2.2 Procedure

A program was written in Matlab to interface with SuperNEC and iteratively perform the simulations. The procedure was as follows:

1) The number of turns of the QHA was set. Simulations were done for 1 - 8 turns.
2) The pitch of the QHA was set. SuperNEC requires all parameters in metres so a conversion from λ to m was performed before setting the parameter.
3) The radius of the QHA was set. SuperNEC requires that the circumference rather than the radius is set so a conversion from radius to circumference was performed before setting the parameter.
4) The simulation was set to provide 2D and 3D radiation patterns as well as VSWR data.

All simulations were performed using an ideal ground plane. As the antenna was designed for a set frequency of 2.245GHz all analysis is for this frequency but results are presented in terms of wavelength (λ).

Kilgus showed that useful results for the Backfire Quadrifilar Helix were found for an approximate region between P = 0.3λ and 0.8λ and R = 0.01λ and 0.12λ [2]. A range extending slightly beyond this range was therefore chosen for simulation. The QHA was simulated with 2 to 8 turns. For each number of turns the QHA was simulated for pitches of 0.1λ to 0.9λ in steps of 0.1λ and radii of 0.01λ to 0.9λ in steps of 0.01λ

A.3 Discussion

When the antennas are grouped according to "usefulness" the above results become more clear. The results were separated into groups by the number of turns. The radiation patterns were classified into three categories namely *Good for General Use*, *Possible Use for Satellite Communications* and *Not useful*.

Good for General Use: These radiation patterns were smooth with minimal side or back lobes present.

Possible Use for Satellite Communications: These radiation patterns had the optimal shape for this application. That is they had a peak magnitude at approximately 60° and a minimum at 0°.

Not Useful: These radiation patterns were either very rippled or distorted or had very large sidelobes and would not be useful for any application.

The results were plotted in groups according to the number of turns of the QHA. The results can be seen in Figures A.2 to A.8. The "Good for General Use" antennas are designated by a '+' and the "Possible Use for Satellite Communications" antennas are designated by a '•'. Antennas that would not be useful were not plotted on the graphs. It should be noted that the VSWR of these antennas is not taken into account when describing them as "useful". The description merely refers to the usefulness of the radiation pattern.

A.3.1 Observations

There is a definite correlation between the number of turns of the antenna and the number of useful radiation patterns it is possible to achieve by varying the pitch and radius. The antennas with a lower number of turns had a higher number of useful results (both for general and satellite use) than those with a higher number of turns.

For N=2 turns, shown in Figure A.2, the number of results suitable for both general and satellite use was high. A point is reached however where there are clearly no more useful results. This point can be described by the line $y = -1.25x + 0.765$.

For N =3 turns, shown in Figure A.3, there is a high number of useful antennas found but fewer than for N=2 turns. Once again there is a definite line, $y = -1x + 0.66$, where the point of no useful results can be

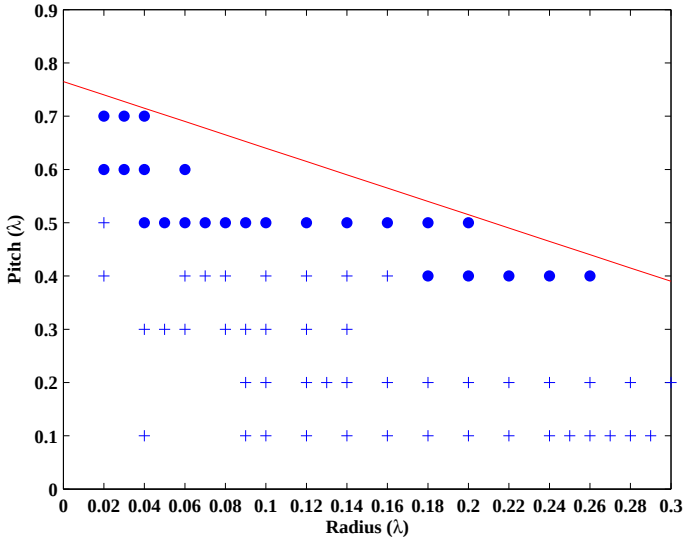

Figure A.2: Results for N=2 Turns

drawn. This line has a lower y-intercept(pitch), thus excluding a larger portion of the simulations from the "useful" area of the graph.

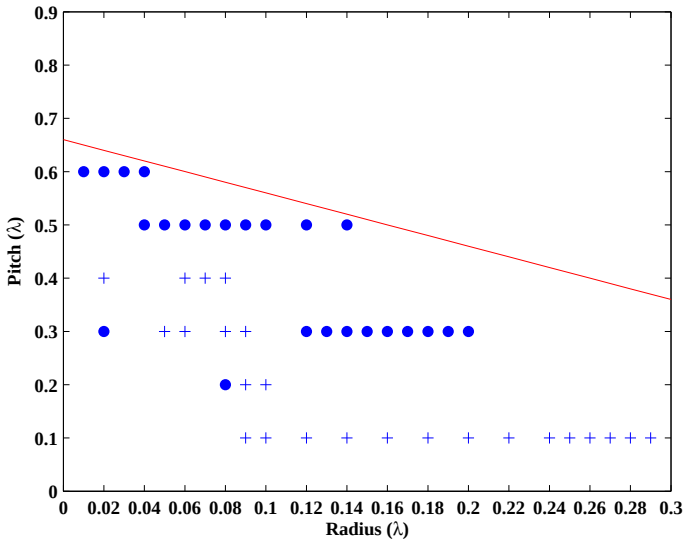

Figure A.3: Results for N=3 Turns

For N = 4 turns, shown in Figure A.4 there is still a large number of antennas that would be useful for general applications. The number of useful antennas for Satellite communications has decreased substantially however. The overall number of useful antennas is less than N=3 turns. The line separating the useful and not useful sections is $y = -0.85x + 0.64$ once again showing a decrease in the y-intercept and hence a smaller area of "usefulness" of the antenna.

For N = 5 turns, shown in Figure A.5, the number of antennas suitable for general use has substantially reduced while the number of antennas suitable for satellite communications has stayed constant. The line separating the useful area is $y = -1.4x + 0.64$ but there is a "dead zone" of poor results between R= 0.15λ and 0.24λ.

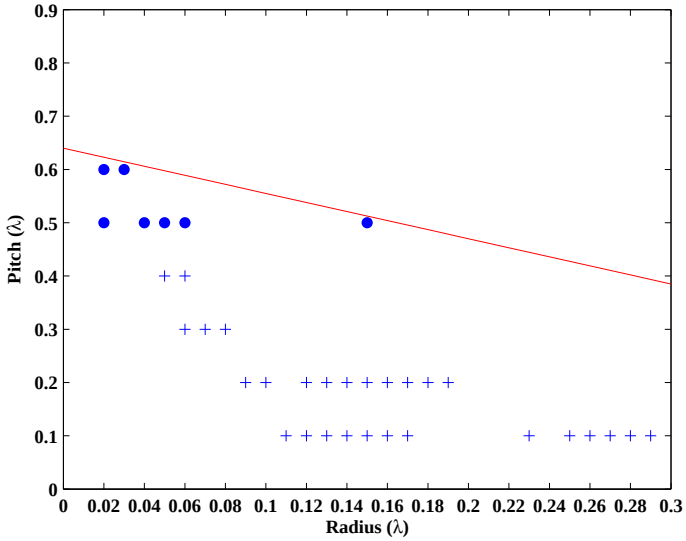

Figure A.4: Results for N=4 Turns

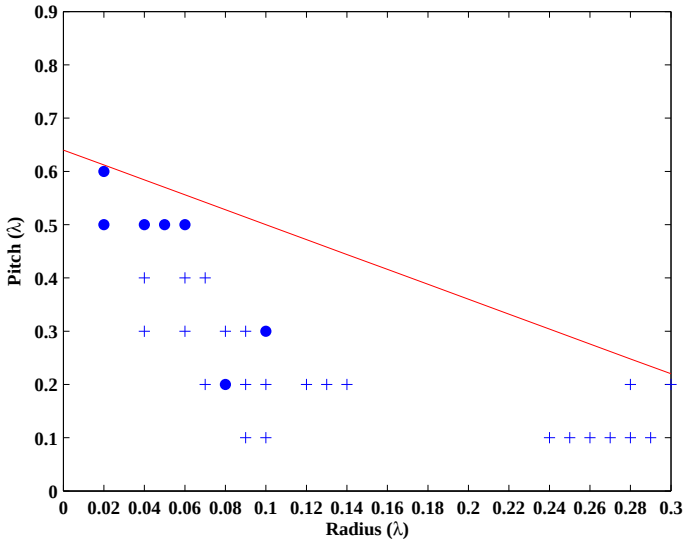

Figure A.5: Results for N=5 Turns

For N = 6 turns, shown in Figure A.6, the number of useful results has significantly reduced. All useful antennas found beyond the "dead zone" described for N=5 turns are no longer useful for either satellite communications or general use. The line separating the areas of usefulness, $y = -2.01x + 0.61$, is steeper and has a lower y-intercept, further reducing the area of "usefulness" of the QHA.

For N = 7 turns, shown in Figure A.7, there are once again useful results beyond P=0.24λ but the "dead" zone is once again present between P=0.17λ and 0.24λ. The number of useful results is significantly reduced compared to N=6 but the line separating the useful and poor performance areas, $y = -1.65x + 0.58$, has a less steep slope.

For N = 8 turns, shown in Figure A.8, the number of useful results is comparable with the antennas with 7 turns. The "dead" zone has shifted to between P=0.13λ and 0.2λ. The line that separates the areas of useful and poor performance, $y = -1.54 + 0.575$, is similar to that for N=7 turns.

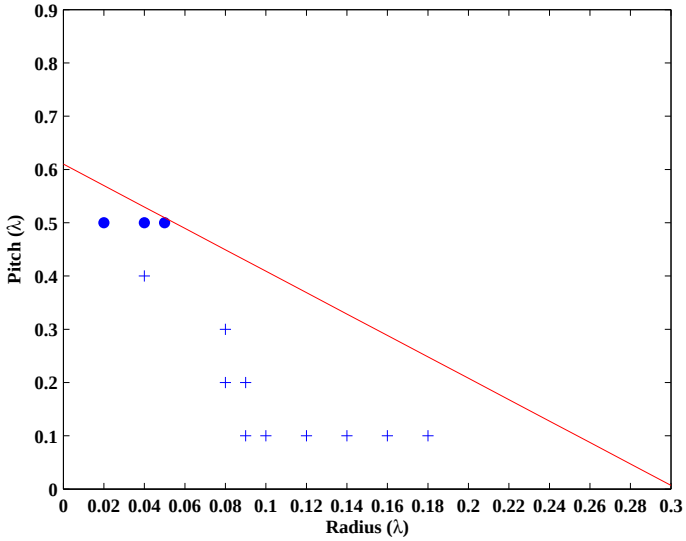

Figure A.6: Results for N=6 Turns

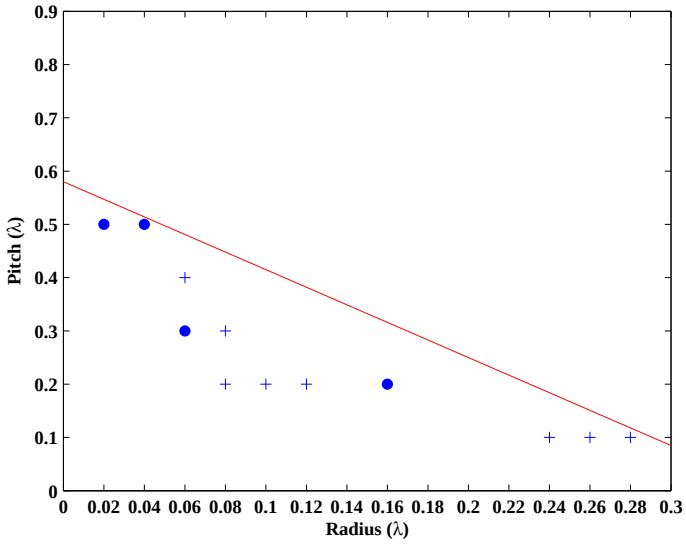

Figure A.7: Results for N=7 Turns

A.3.2 VSWR

The VSWR behaviour of the QHA was less predictable than the radiation patterns but there were some trends noted. The VSWR improved as the radius and pitch of the antenna increased. The QHAs with higher number of turns had poorer VSWRs. This is most likely due to the fact that an antenna with many turns and that is narrow and with lower pitch has more elements closer together. This would increase the capacitive component of the antenna and therefore increase the VSWR.

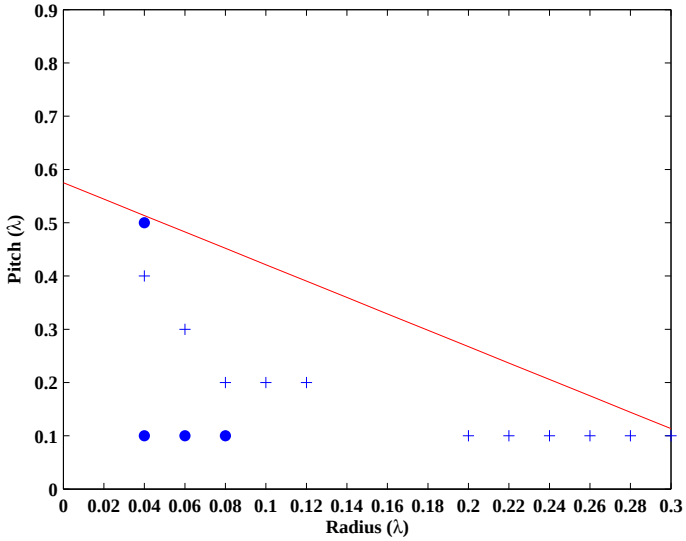

Figure A.8: Results for N=8 Turns

A.4 Summary of Results

From the above results it can be seen that the performance of the quadrifilar helix is greatly affected by the number of turns, pitch and radius. The number of useful results is largely determined by the number of turns of the QHA. The QHAs with more than 6 turns produced a lot fewer useful results, both for general and satellite use, than those with less than 6 turns. It should be noted at this point that it is not essential for the QHA to have an integral number of turns (as in the resonant quadrifilar helix antenna) [3]. In order to reduce the number of simulations for this analysis only integral numbers of turns were chosen.

A line can be drawn separating the areas of the graph where useful results can be found and where the radiation patterns become of little use due to distortion,ripples and/or sidelobes . The area above this line increases as the number of turns increase. The y-intercept of this line decreases with the number of turns of the QHA. This, in turn, lowers the area of the graph which produces acceptable radiation patterns.

The usefulness of the QHA (ie whether or not it produced a radiation pattern with a maximum on the edge) is largely determined by the radius and pitch of the antenna. A pattern possibly suitable for satellite communications is more likely to be found on an antenna with a mid to high pitch and small radius. This is, however, less evident for the QHAs with a larger number of turns where the occurance of radiation patterns suitable for satellite communications seems to be a little more “random”.

A.5 Conclusion

The performance of the quadrifilar helix antenna depends on the number of turns, pitch and radius of the QHA. The lower the number of turns the higher the number of useful radiation patterns observed. Pitch values greater than 0.8λ do not, in general, produce useful radiation patterns. The radius does not affect results with as much predictability. This study only observed QHAs with an integral number of turns. A further study into QHAs with a non-integral number of turns would be useful.

References

[1] Poynting Innovations. SuperNEC. www.supernec.com. Last accessed 30 November 2009.

[2] Charles C. Kilgus. Shaped-Conical Radiation Pattern Performance of the Backfire Quadrifilar Helix. *IEEE Transactions on Antennas and Propogation*, May:392–397, 1975.

[3] Charles C. Kilgus. Resonant Quadrifilar Helix Design. *Microwave Journal*, 13:49–54, 1970.

Appendix B

Design of Feed Network for a Quadrifilar Helix Antenna

B.1 Introduction

This document details the different options for use when feeding the Quadrifilar Helix(QHA). The Lange Coupler, Corporate Feed, 90° and 180° Hybrid combination as well as a Wilkinson Splitter were investigated.

B.2 Problem Statement

The quadrifilar helix antenna(QHA) is designed to be fed in phase quaderature [3]. This is to say that each of the four arms of the QHA must be fed 90° out of phase with the arm before it. Therefore if the QHA is fed with a signal of amplitude 'A' then one arm will be fed with a signal $A\angle 0^\circ$, the second with $A\angle 90^\circ$, the third with $A\angle 180^\circ$ and the fourth with $A\angle 270^\circ$.

B.3 Research Conducted

The following four options were investigated as feed networks for the QHA.

- Lange Coupler
- Corporate Feed with Meandering Lines
- 90° and 180° Hybrid Combination
- Wilkinson Splitter with Meandering Lines

The operation of each is described in this section.

B.3.1 Lange Coupler

The Lange coupler, designed by J. Lange, is a microstrip device which uses four coupled lines with interconnections [5]. It is a type of quadrature coupler. This means that there is a 90° phase change between outputs. The circuit can be seen in *Figure B.1* below.

This coupler was not used for the phase splitting, however, due to the fact that it was more complex to manufacture than the other options. Its lines are very narrow and there are cross wires between lines which are difficult to manufacture without specialised equipment.

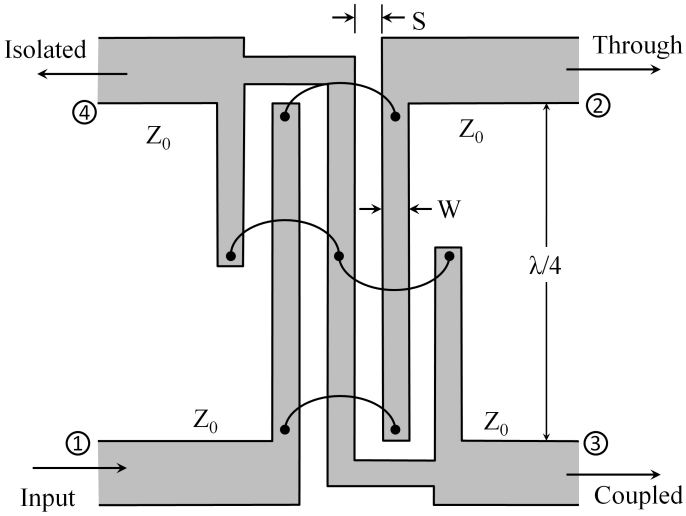

Figure B.1: Lange Coupler [5]

B.3.2 Corporate Feed

The corporate feed network consists of a section of 50Ω line. Connected to this line are four sections of 75Ω line each of $\frac{\lambda}{4}$ long. To enable this feed to include phasing a series of "meandering lines" must be included. At the termination of each 75Ω section 50Ω lines of different lengths are connected. One of $\frac{\lambda}{4}$, one of $\frac{2\lambda}{4}$, one of $\frac{3\lambda}{4}$ and one of 1λ. Each of these would be connected to an arm of the QHA.

B.3.3 90° and 180° Hybrids

A 90° hybrid (also known as a branchline coupler [2]) in combination with a 180° (or rat-race) hybrid would also split the signal with the desired phase shift.

90° Hybrid: This coupler as seen in *Figure B.2* consists of sections of transmission line that form a square or circular shape as follows: two sections of series transmission line $\frac{\lambda}{4}$ long separated by two sections of parallel transmission line $\frac{\lambda}{4}$ long forming either a square of perimeter 1λ as seen in *Figure B.2*, or a circle of circumference of 1λ. Each pair of transmission lines has a specific impedance depending on the coupling desired. For equal magnitude splitting the series arms have a characteristic impedance, $Z_{series} = Z_0$ and the parallel arms have a characteristic impedance, $Z_{shunt} = \frac{Z_0}{\sqrt{2}}$ [2].

180° Hybrid: In order to get the required four outputs from the feed network as a whole a 180° coupler (or rat-race ring [2]) is required with an output to each 90° coupler. This coupler, seen in *Figure B.3*, consists of a ring of circumference 1.5λ with four arms. These arms are separated by $\frac{\lambda}{4}$ and there is a $\frac{3\lambda}{4}$ distance between the outside two arms. Each arm has a characteristic impedance of Z_0 and the circular section has a characteristic impedance of $\sqrt{2}Z_0$. Depending on which arm is used as the input, the coupler can split the signal equally with either a 0° or 180° phase difference [2].

B.3.4 Wilkinson Power Divider

This power splitter designed by E. Wilkinson can be designed to split a signal into any number of equal amplitude, equal phase, signals with isolation between the output terminals [6] ,[5]. The circuit diagram of

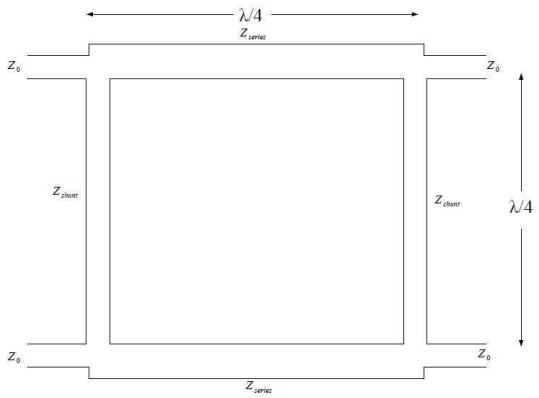

Figure B.2: Branchline Coupler

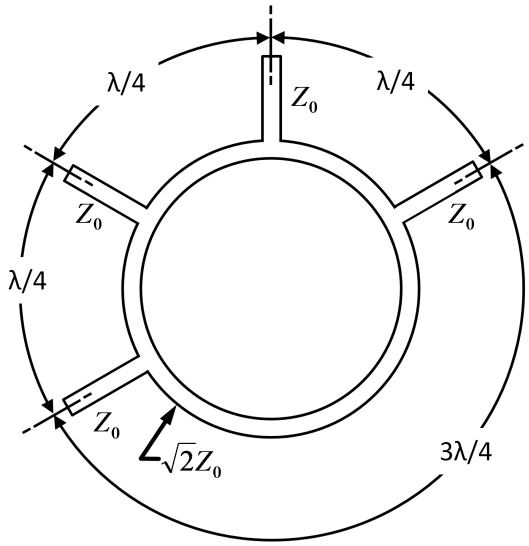

Figure B.3: 180° Hybrid

a two way Wilkinson Power Divider can be seen in *Figure B.4*. For the purposes required here a 4-way splitter could be designed. This, however, would require crossovers [5] which are more difficult to fabricate. For this reason a network of three, 2-way splitters was designed. In order to realise the required phasing a series of transmission lines, as in the Corporate Feed described above, would be required.

B.4 Design Notes

The Corporate Feed and 90°-180° hybrids feed networks were all designed and constructed for use at 2.245GHz. They were constructed on FR-4 for which the permittivity, ϵ_r, was assumed to be 4.4. The microstrip line on the FR-4 was designed to have the required characteristic impedances for each section of each feed network.

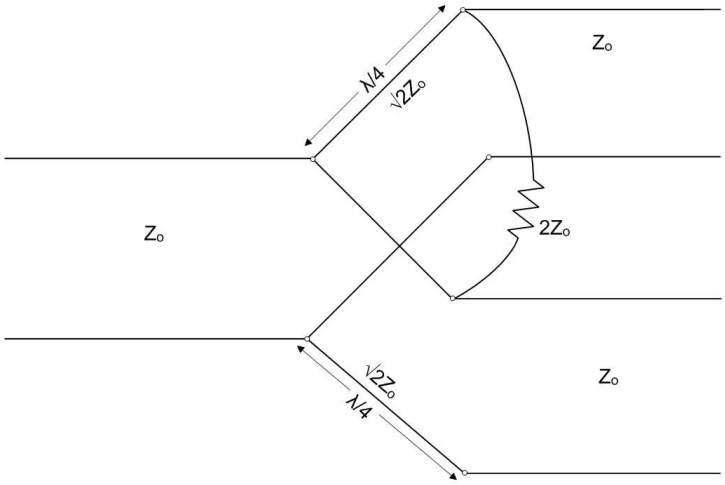

Figure B.4: Wilkinson Power Divider

B.5 Creating Microstrip Line with a Specific Characteristic Impedance

For each of these circuits a specific characteristic impedance, Z_0, and line length are required. These parameters are set by adjusting the height to width ratio of the microstrip line, taking into account the materials used and frequency of operation [5].

The characteristic impedance of a microstrip transmission line can be determined by its width to height ratio. In order to find the correct ratio for the desired Z_0 a series of equations need to be satisfied. These start with the given permittivity ϵ_r of the board in question. In this case it is FR-4 and the permittivity was assumed to be 4.4. ϵ_r changes (to ϵ_{eff}) due to the width to height ratio of the microstrip line according to equation B.1 or B.3

Therefore, in order to obtain the desired Z_0 an iterative process must be followed using equations B.1 and B.2.

These equations, designed by Gardiol [4] are set for two cases: when the width to height ratio of the microstrip line is less than 1 and when it is greater than or equal to 1.

For w/h < 1

$$\epsilon_{eff} = \frac{\epsilon_r + 1}{2} + \frac{\epsilon_r - 1}{2}\left(\frac{1}{\sqrt{1 + \frac{12}{w/h}}} + 0.04(1 - w/h)^2\right) \tag{B.1}$$

and

$$Z_0 = \frac{60}{\sqrt{\epsilon_{eff}}} \ln\left(\frac{8}{w/h + \frac{w/h}{4}}\right) \tag{B.2}$$

For the case where w/h ≥ 1

$$\epsilon_{eff} = \frac{\epsilon_r + 1}{2} + \frac{\epsilon_r - 1}{2} \left(\frac{1}{\sqrt{1 + \frac{12}{w/h}}} \right) \tag{B.3}$$

and

$$Z_0 = \frac{120\pi}{\sqrt{\epsilon_{eff}}} \div (w/h + 1.393 + 0.667 \ln (w/h + 1.444)) \tag{B.4}$$

The iterative process of finding the parameters of the microstrip line for a desired Z_0 were as follows:

An approximate w/h was chosen and Z_0 calculated. Depending on whether Z_0 was too low or too high a new w/h was chosen and Z_0 calculated again. This process was repeated until the desired Z_0 was found.

ϵ_{eff} also affects the velocity of the wave propagating through the FR-4. This has an effect on the wavelength of the signal. This is a very important observation as the 90° and 180° Hybrids require very specific transmission line lengths. The velocity of the wave can be found using equation B.5

$$v = \frac{c}{\sqrt{\epsilon_{eff}}} \tag{B.5}$$

Where:

v :	velocity of the wave in m/s
c :	speed of light in m/s
ϵ_{eff} :	Effective permittivity

Using this velocity the wavelength, λ, can be found using equation B.6

$$\lambda = \frac{v}{f} \tag{B.6}$$

Where:

λ :	wavelength in m
v :	velocity of propagation through medium in m/s
f :	frequency in Hz

Under these conditions a quarter wavelength line on FR-4 of permittivity of 4.4 at 2.245GHz has the following properties:

Characteristic Impedance, $Z_0(\Omega)$	w/h	Width(mm)	Length of $\frac{\lambda}{4}$(mm)
50Ω:	1.9125	3.06	18.3
35.4Ω	3.27	5.232	17.9

B.6 90° and 180° Hybrids

For the 90° hybrid an equal power split with 90° phase difference is required. For this case the series arms must have a characteristic impedance Z_0=35.4Ω and the shunt arms have Z_0=50Ω[2] with the input and output arms having a Z_0=50Ω characteristic impedance.

Therefore, using Equations B.1- B.6, the circuits shown in *Figure B.5* to *Figure B.7* were designed to have the following parameters:

Branchline Coupler:

- $\frac{\lambda}{4}$ long 50Ω branches: width=3.06mm, length=18.3mm
- $\frac{\lambda}{4}$ long 35.4Ω branches: width=5.232mm, length=17.9mm

The ground arm of each BLC was taken to ground via a 50Ω resistor.

Each BLC was fed by an arm of the 180° coupler Hybrid Ring Coupler:

- 70.7Ω sections: width=1.6mm, length=112.53mm

B.7 Corporate Feed

The corporate feed network was designed to have the properties described. The widths and lengths of transmission line were found using Equations B.1- B.6.

The $\frac{\lambda}{4}$, 75Ω sections have a width of 1.42mm and length of 18.83mm. The meandering lines have the following properties:

Electrical Length	Physical Width(mm)	Physical Length(mm)
$\frac{\lambda}{4}$	3.06	18.3
$\frac{\lambda}{2}$	3.06	36.6
$\frac{3\lambda}{4}$	3.06	54.9
1λ	3.06	73.2

B.8 Wilkinson Splitter

In order for the desired phase shift to be achieved an arrangement of Wilkinson Splitters together with phased lengths of transmission lines is required. The Wilkinson Splitters divide the signal into four, equal magnitude signals and the transmission lines of length $\frac{\lambda}{4}$, $\frac{\lambda}{2}$, $\frac{3\lambda}{4}$ and 1λ ensure that each signal is 90° out of phase with the next when it is fed to the QHA.

The design consisted of three Wilkinson Dividers. A first divider splits the signal into two equal signals and then each of these signals is fed into one of two further Wilkinson Dividers which splits it into two equal signals once again. The original input signal is therefore divided into four equal magnitude and phase signals. The characteristic impedance of the arms of the splitter is found according to Equation B.7, below.

$$Z = \sqrt{2}Z_0 \tag{B.7}$$

Therefore for the Wilkinson Divider to have a total Z_0 of 50Ω its arms must have a characteristic impedance of 70.7Ω.

Using Equations B.1- B.6 on a board of FR-4 of height 1.6mm the microstrip line was required to have a width of 1.33mm and a $\frac{\lambda}{4}$ length of 17.22mm.

Between each of these arms there is an isolation resistor whose magnitude is determined by Equation B.8, below.

$$R = 2Z_0 \tag{B.8}$$

Therefore for the desired Z_0 of 50Ω the isolation resistor must be equal to 100Ω. When constructed chip resistors were used due to the high frequency of operation.

Using Equations B.1- B.6 the lengths of the phasing transmission lines were found to be as follows:

Electrical Length	Physical Width(mm)	Physical Length(mm)
$\frac{\lambda}{4}$	2.62	16.78
$\frac{\lambda}{2}$	2.62	33.56
$\frac{3\lambda}{4}$	2.62	50.35
1λ	2.62	67.13

The final circuit can be seen in *Figure B.7* below.

B.9 Construction

The feed networks were constructed by etching out the microstrip lines on a board of FR-4. The circuits were designed using the PCB layout program EAGLE. The etching technique used was a subtractive process. The outline of the circuit was cut out using a circuit etching machine at the University of the Witwatersrand. The extra copper was then peeled off revealing the circuits. *Figure B.5* shows the Hybrid ring, branchline coupler combination. *Figure B.6* shows the Corporate Feed network and *Figure B.7* shows the Wilkinson splitter feed network.

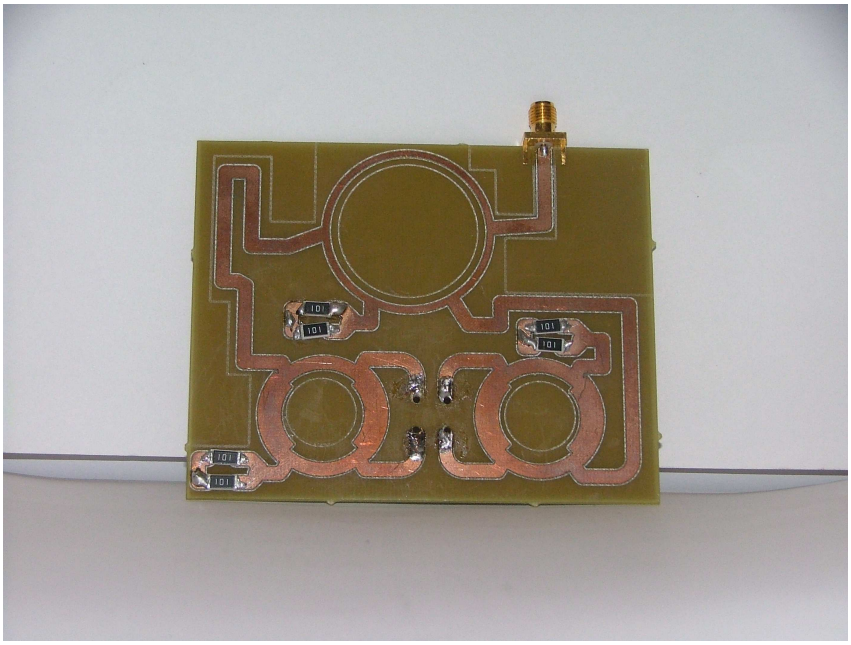

Figure B.5: 180° and 90° hybrid combination

B.10 Discussion

The corporate and 90-180° feed networks were constructed first. When the unit (feed network, antenna and connectors) was assembled and tested the results were not optimal. The radiation pattern was not as balanced as expected and the gain of the antenna was much lower than expected. For this reason a set of tests discussed in Appendix C, [1], were performed to determine the velocity factor of the FR4 and hence the permittivity of the FR4. These values were then used for the Wilkinson splitter. The results of the Wilkinson splitter were significantly better with a more balanced radiation pattern and higher gain, although still not as high

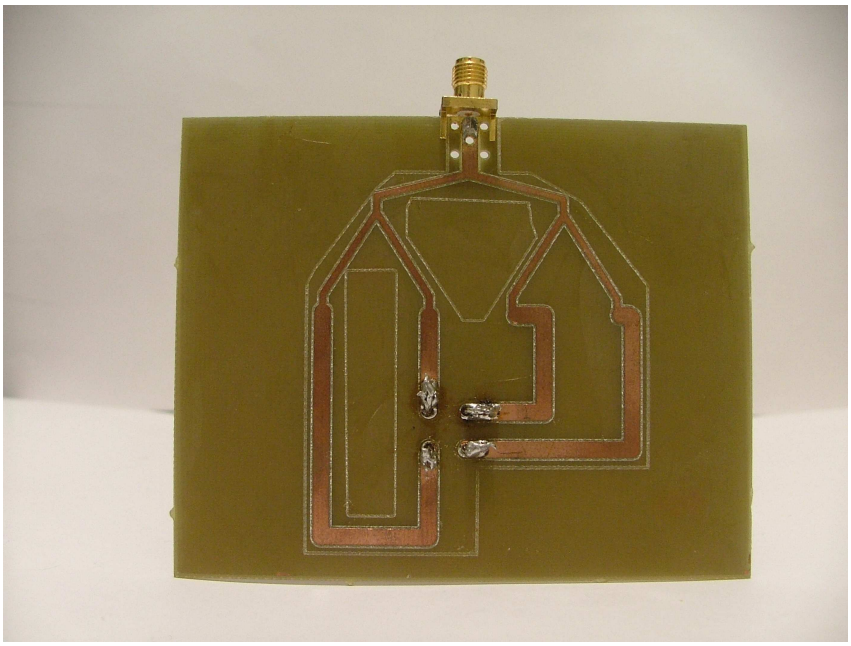

Figure B.6: Corporate Feed

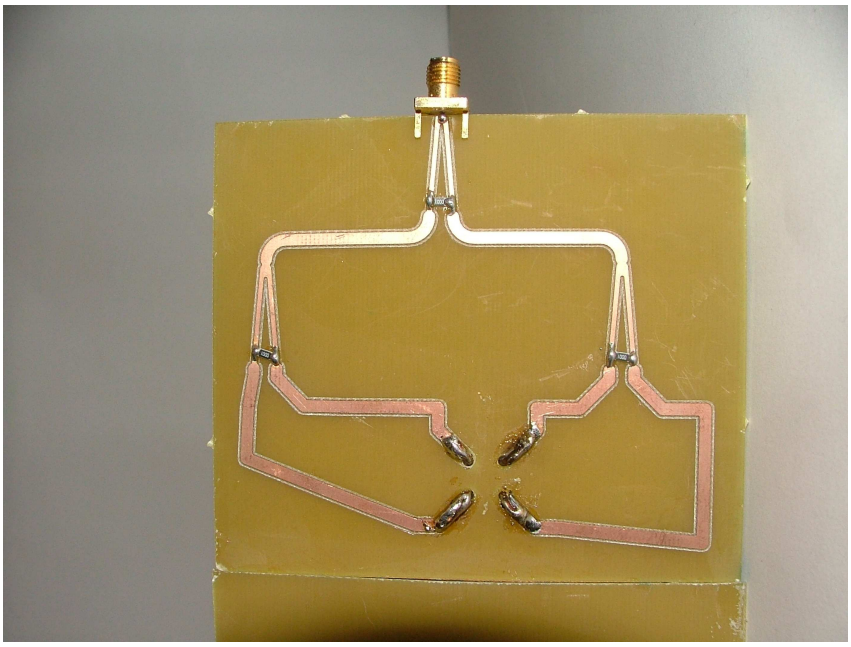

Figure B.7: Wilkinson Splitter

as expected. This shows that the use of the correct permittivity in the equations is of very high importance in order to achieve correct results.

B.11 Conclusion

Three feed networks were designed and built: a corporate feed network, 90-180° combination and a Wilkinson splitter. Tests were performed on the FR-4 used for the circuits to most accurately determine its permittivity and velocity factor. The Wilkinson splitter arrangement showed the most accurate performance with the unit

with this feed network giving the radiation pattern closest to that expected from simulations.

References

[1] Heather Fraser. Appendix C - Construction and Testing. M.Sc, University of the Witwatersrand, 2009.

[2] Harlan Howe Jr. *Stripline Circuit Design*. Artech House, 1985.

[3] Charles C. Kilgus. Resonant Quadrifilar Helix Design. *Microwave Journal*, 13:49–54, December 1970.

[4] Personal Communication. Prof Alan Clark. University of the Witwatersrand, May 2008.

[5] David M Pozar. *Microwave Engineering*. John Wiley and Sons, Inc, 1998.

[6] Ernest J Wilkinson. An N-Way Hybrid Power Divider. *IRE Transactions on Microwave Theory and Techniques*, 8(2):116–118, January 1960.

Appendix C

Construction and Testing

C.1 Introduction

This document details the construction and testing of a Quadrifilar Helix Antenna (QHA). The QHA was designed for use at 2.245GHz and was required to have a radiation pattern with a higher gain at approximately 60° than at 0°.

C.2 Design

C.2.1 Design of Quadrifilar Helix Antenna

A series of Quadrifilar Helices were simulated using SuperNEC. These simulations can be found in [1]. The best of these simulations were looked at and refined. The most suitable results for the purpose required were at a pitch of 0.6λ and radius of 0.03λ on a QHA with 3 turns. In order to find the optimal antenna to be built, further simulations were performed at finer iterations around this area. The results found can be seen in Table C.1.

Table C.1: Further simulations for N = 3 Turns and Pitch = 0.6 λ

Radius(λ)	Centre Gain(dB)	Edge Gain(dB)	VSWR
0.031	-1.85	6.18	1.54:1
0.032	-2.0	6.18	1.36:1
0.033	-2.1	6.17	1.21:1
0.034	-2.25	6.16	1.07:1
0.035	-2.4	6.11	1.10:1
0.036	-2.51	6.10	1.23:1
0.037	-2.61	6.08	1.37:1
0.038	-2.67	6.06	1.52:1
0.039	-2.74	6.05	1.69:1

The antenna with the lowest VSWR was chosen for construction. Therefore the constructed antenna had the following parameters:

Number of turns = 3
Pitch = 0.6λ
Radius = 0.034λ

These specifications are all in wavelengths. Converted to milimetres the antenna has the following specifications:

Pitch = 80.18mm
Diameter = 9.09mm

C.2.2 Design of Feed Network

Three feed networks were designed for use with the QHA. These were a corporate feed network, 90°-180° hybrid combination and a Wilkinson divider arrangement. The full detail of these designs can be found in [2].

C.3 Construction

C.3.1 Materials

The structure was made out of easily available materials that were as inexpensive as possible. The QHA was constructed out of 1mm thick copper wire and the feed network consisted of copper microstrip line on a board of FR-4. The resistors used were chip resistors as these perform better at high frequencies than wire wound or carbon resistors [3].

C.3.2 Procedure

The antenna was wound around a piece of cardboard wrapped around a wooden dowel. As the diameter of the QHA had to be 9mm an 8mm dowel was used. The cardboard was approximately 0.5mm thick so this contributed the final 1mm diameter. The pitch of the antenna was marked out on the cardboard and this was then wrapped around the dowel and secured with masking tape. One piece of copper wire was wrapped around this arrangement, carefully following the markers drawn. This wire would make up the one bifilar of the quadrifilar helix (ie two helices). Being sure not to dislodge the first bifilar a second bifilar was wound in the same manner. The two bifilars crossed at the top of the dowel. The insulation on the wire at this point was rubbed off and the crossovers were soldered together. The structure was secured with cable ties and left undisturbed for approximately two days. This was in order to ensure that the QHA kept its shape once removed from the dowel.

The cardboard and antenna structure were removed from the dowel. Due to the thick wire used and the support of the cardboard the antenna structure retained its shape.

This arrangement was then connected to the feed network by inserting the ends of the bifilars through holes drawn in the board and soldering them directly onto the feed network. In some instances the cardboard was cut out and removed from the QHA and in others it was not. This was to see whether or not it would have an effect on the radiation pattern of the QHA.

A new antenna structure was constructed for each feed network. *Figure C.1* shows the constructed QHA with the cardboard support in place and *Figure C.2* shows the constructed QHA without the cardboard support in place.

C.4 Testing

The QHA was tested in the anechoic chamber at the University of the Witwatersrand, Johannesburg. The antenna and feed network were connected to a Hewlett Packard network analyser and measurements taken of VSWR and S_{21} (which was converted to gain). The antenna was placed on a rotating mast and measurements were taken at 5° intervals so as to give a radiation pattern.

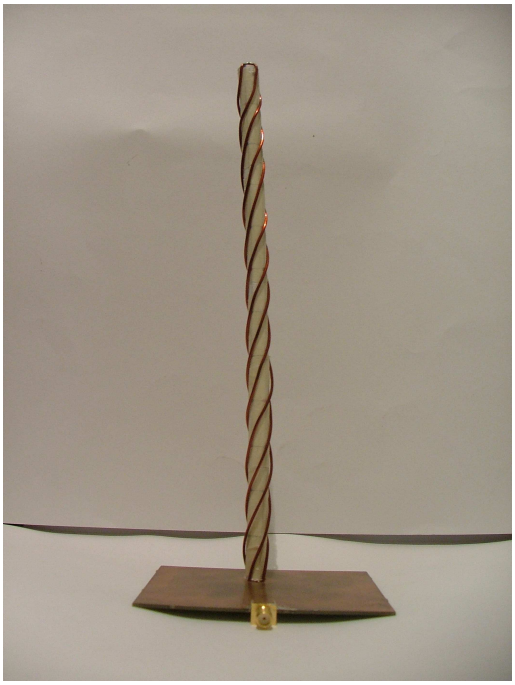

Figure C.1: QHA with cardboard support

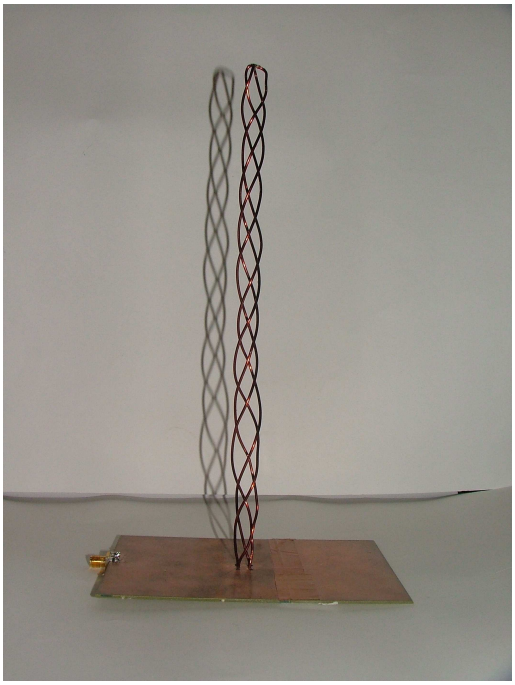

Figure C.2: QHA with no cardboard support

C.5 Results- Corporate Feed and 90°-180° Hybrid Feed

Measurements were taken for the QHA with each of the feed networks (Corporate feed, 90°-180° Hybrids and Wilkinson Splitter). These were then converted into radiation patterns which can be seen below.

The QHA with the Corporate feed network shows the poorest performance. There is a definite drop in gain towards 0° but the gain is approximately 8dB lower than that predicted and there are sidelobes present. The graph of gain versus angle can be seen in *Figure C.3.*

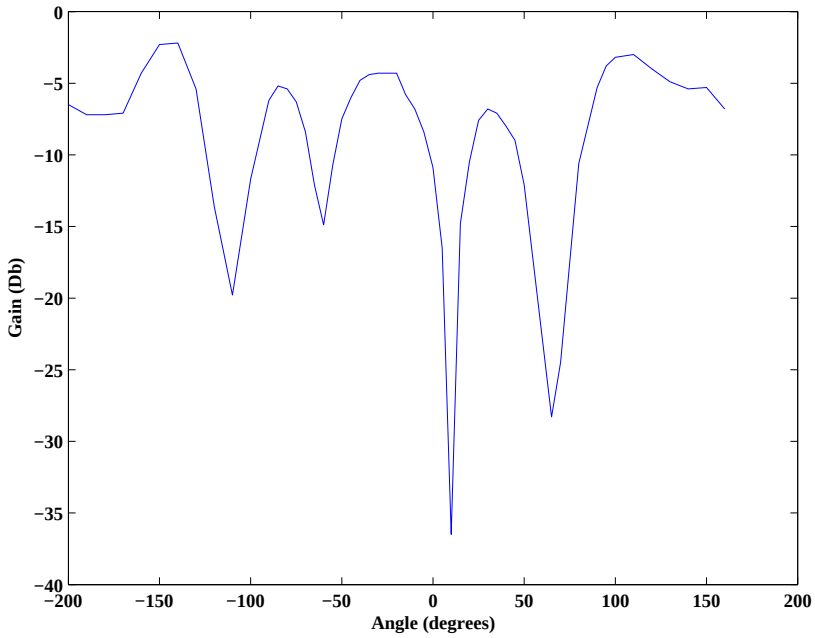

Figure C.3: Radiation Pattern of Corporate Feed Fed QHA.

The 90°-180° hybrid combination showed a slightly better performance with a more symmetrical radiation pattern with a depression at approximately 0°. The gain is still approximately 10dB lower than expected. The graph of gain versus angle can be seen in *Figure C.4.*

C.6 Discussion

The results show both good and bad properties. The radiation pattern is shaped very much like the simulations expect it to. There is a definite maximum at between 50° and 60° and minimum at approximately 0°.

The gain of the QHA does not, however, compare favourably to the simulation. The gain is between 10dB (worst case) and 6.4dBs (best case) lower than predicted. This was first noted on the antennas using the corporate and 90°-180° hybrid feed networks. It was thought that the feed network may be the source of the loss.

The characteristic impedance of the various sections of microstrip line making up these feed networks is of great significance and it is therefore a factor that could possibly affect the performance of the feed network and consequently the gain of the antenna as a whole. Therefore before the Wilkinson splitter was constructed a series of tests were performed to more accurately determine the velocity factor of the FR-4 being used as well as the characteristic impedance of various widths of transmission line.

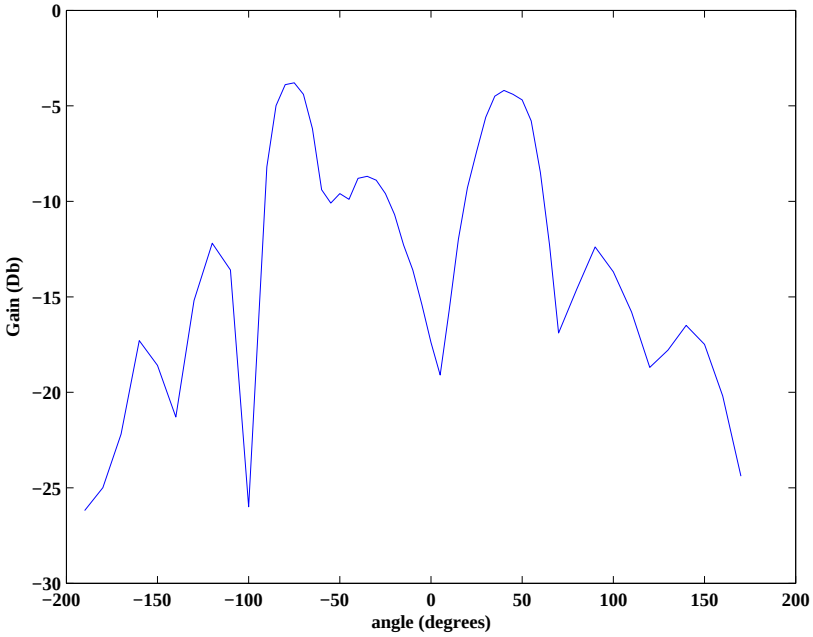

Figure C.4: Radiation Pattern of 90°-180° hybrid Feed Fed QHA.

C.7 Tests on Characteristic Impedance of Microstrip Line

As discussed in Section 6, above, the exact characteristics of the microstrip line of the feed network needed to be ascertained. In order to do this a number of tests were performed.

A series of transmission lines of various widths and lengths were milled out on a board of FR-4 of the same type and make as that used for the original feed networks. An open circuit test and a short circuit test were performed on the various transmission lines at various frequencies.

Using Equation C.1 Z_0 could be found for the lengths of transmission line.

$$Z_0 = \sqrt{Z_{oc} Z_{sc}} \tag{C.1}$$

It was found that this Z_0 varied greatly with frequency. For a transmission line with width 2mm the characteristic impedance varied according to Table C.2. As can be seen in Table C.2 the characteristic impedance is close to 50Ω at low frequencies but deviates from this value at higher frequencies.

Table C.2: Variation of Z_0 with Frequency

Frequency	$Z_0(\Omega)$
567 MHz	51.40+0.6 j
1.3 GHz	57.03 +0.38 j
2.02 GHz	73.77-0.13 j
2.32 GHz	19.7993 + 2.2072j
2.58 GHz	108.31-81.9 j

It was therefore concluded that the incorrect value of permittivity had been used for the calculations of characteristic impedance for the Corporate feed network and 90°-180° hybrids. The correct value could be found from the velocity factor of the medium and used in the Wilkinson splitter arrangement to give better results.

To find the correct velocity factor for the transmission line the physical and electrical lengths of the microstrip transmission line were compared. Two sections of transmission line were milled on the same sample of FR-4 to be used for the Wilkinson splitter. The difference in physical length of the two lines was 8.7mm. The difference in electrical length between the two lines as observed on a smith chart was 0.13λ and at 2.245GHz this translates to 0.0174m. By substituting these values into Equation C.2 the velocity factor was found to be 0.5.

$$VF = \frac{l_{phys}}{l_{elec}} \tag{C.2}$$

The effective permittivity ϵ_e is found by Equation C.3 to be 4.0.

$$\epsilon_e = \frac{1}{VF^2} \tag{C.3}$$

Using the equations described in [2] and substituting the above information the Wilkinson splitter was designed as described in [2].

C.8 Results-Wilkinson Power Divider Arrangement

The best performing of all feed networks was the Wilkinson splitter arrangement. The shape of the radiation pattern is directly comparable to that obtained in simulation. Two sets of measurements were taken. *Figure C.5* shows the results for the QHA without the cardboard support. The presence of the cardboard support affects the gain of the QHA as the antenna without the support has a gain of 3.5dB higher, on average, than that with the cardboard support.

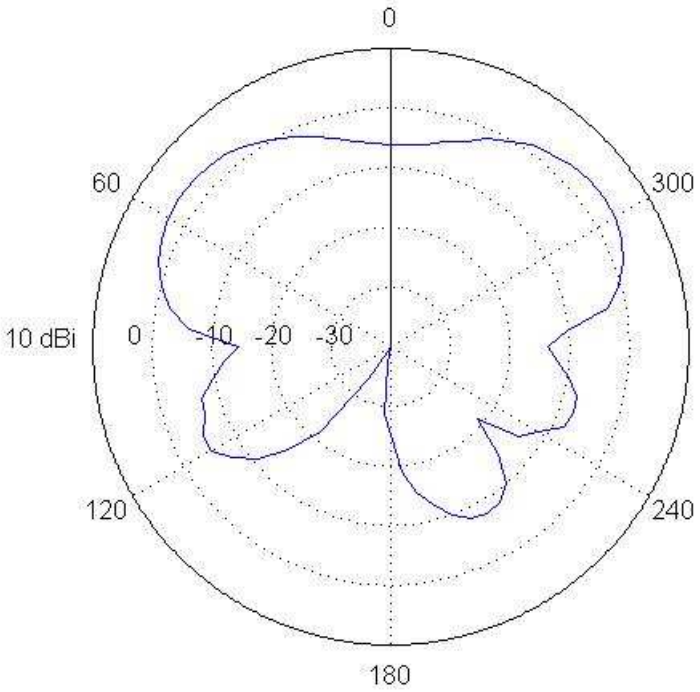

Figure C.5: Radiation Pattern of Wilkinson splitter Feed Fed QHA.

The results show that the radiation pattern produced agreed better with the expected results than the corporate

feed and 90°-180° hybrid combination. This was likely due to a more balanced input to the antenna which was in turn caused by the more accurate Z_0 as well as the greater isolation [4] between outputs of the Wilkinson power divider.

C.9 Recommendations on Future Work

It is recommended that more research is conducted into the feed networks described. The lower gain of the QHA could very possibly be due to the poor performance of the feed networks. A higher accuracy circuit etching method should be used to construct the feed networks as the inaccuracy of the one used for this research is possibly affecting the performance of the feed network and hence the antenna as a whole.

C.10 Conclusion

The QHA was built and tested with three different feed networks: a Corporate Feed Network, a 90°-180° hybrid combination and a Wilkinson Power divider arrangement. The best performing of these three was the Wilkinson Power Divider arrangement.

References

[1] Heather Fraser. Appendix A - Simulations and Results. M.Sc, University of the Witwatersrand, 2009.

[2] Heather Fraser. Appendix B - Design of Feed Network for a Quadrifilar Helix Antenna. M.Sc, University of the Witwatersrand, 2009.

[3] Personal Communication. Professor Alan Clark. Wits University, September 2008.

[4] Personal Communication. Derek Nitch. Poynting Antennas, November 2008.

Appendix D

Simulations and Results

D.1 Results

This section presents the results obtained from simulation of the QHA as described. Although pitches of 0.9λ were simulated none of the combinations of turns and radii gave any useful results at this pitch or higher. The results are therefore omitted from the tables of results presented here. In some tables the results for every other radius (ie. 0.02λ, 0.04λ etc.) are presented. In these cases there was little to no change at the omitted radius and so the result is not presented here.

A radiation pattern that is described as having a good "general" shape or behaviour has a smooth pattern which would be suitable for an application that would not require a specialised shape.

While simulations were observed in increments of Pitch 0.1λ if the results did not vary significantly between simulations only one set of simulation results is presented here.

D.1.1 Results for N = 2 Turns

Good general behaviour was noted within pitches of 0.1λ to 0.5λ.

D.1.1.1 Pitch= 0.1 λ

At 0.1λ the pattern was not rippled and there were no instances of multiple lobes for radii of 0.04λ to 0.3λ. Some very poor VSWRs were noted and can be seen in Table D.1.

Table D.1: Results for N=2, P=0.1 λ

Radius(λ)	**Shape of Pattern and Comments**	**Maximum Gain(dB)**	**Gain at centre if applicable(dB)**	**VSWR**
0.04	Normal beam	-6.8	-	27.7:1
0.06	Wider beam	-8.6	-	105:1
0.08	Narrow beam	-8.4	-	24:1
0.1	Normal beam, 46°HPBW	5.2	-	25.5:1
0.12	Smooth beam, 44°HPBW	7.8	-	2.13:1
0.14	Smooth beam, 44°HPBW	8.4	-	4.99:1
0.16	Smooth beam, 43°HPBW	8.8	-	2.68:1
0.18	Smooth beam, 45°HPBW	9.1	-	3.05:1
0.2	Smooth beam, 43°HPBW	9.0	-	6.39:1
0.22	Smooth beam, 43°HPBW	8.5	-	11.7:1
0.24	Smooth beam, 45°HPBW	8.2	-	19.1:1
0.26	Smooth beam, 35°HPBW	9.9	-	24.8:1
0.28	Smooth beam, 38°HPBW	8.9	-	33.1:1
0.3	Smooth beam, 46°HPBW	8.3	-	40:1

D.1.1.2 Pitch = 0.2λ

At 0.2λ acceptable patterns suitable for general use were found between radii of 0.06λ and 0.26λ. VSWR performance was better than at 0.1λ but there were still some unacceptably high values. These results can be seen in Table D.2.

Table D.2: Results for N=2, P=0.2 λ

Radius(λ)	**Shape of Pattern and Comments**	**Maximum Gain(dB)**	**Gain at centre if applicable(dB)**	**VSWR**
0.02	Wide, smooth beam	-2.4	-	99:1
0.06	Smooth beam, 30°HPBW	5.2	-	58.5:1
0.08	Smooth beam, 34°HPBW	8.4	-	27.5:1
0.1	Smooth beam, 60°HPBW	5.5	-	7.17:1
0.12	Smooth beam, 65°HPBW	4.86	-	2.67:1
0.14	Wide beam, depression at 0°	4.64 at $\pm$40°	3.85	5.3:1
0.16	Wide beam, depression at 0°	4.84 at $\pm$45°	2.82	2.59:1
0.18	Wide beam, depression at 0°	5.08 at $\pm$45°	2.62	2.26:1
0.2	Wide beam, depression at 0°	5.26 at $\pm$47°	2.13	5.95:1
0.22	Wide beam, depression at 0°	5.28 at $\pm$51°	2.44	2.17:1
0.23	Smooth beam	4.25	-	2.59:1
0.24	Smooth beam, 61°HPBW	6.5	-	8.38:1
0.26	Smooth beam, 41°HPBW	8.1	-	3.08:1
0.28	Smooth beam, 61°HPBW	6.2	-	10.5:1
0.3	Smooth beam, 71°HPBW	5.8	-	3.72:1

D.1.1.3 Pitch = 0.3λ

At 0.3λ acceptable patterns suitable for general use were found between 0.04λ and 0.14λ. From 0.16λ to 0.3λ more ripple was evident in the radiation patterns. Good VSWR was noted at 0.1λ, 0.22λ and 0.26λ. All results can be seen in Table D.3.

Table D.3: Results for N=2, P=0.3 λ

Radius(λ)	**Shape of Pattern and Comments**	**Maximum Gain(dB)**	**Gain at centre if applicable(dB)**	**VSWR**
0.04	Wide beam, 40°HPBW, slight side-lobes	5.61	-	112:1
0.06	Smooth beam, 39°HPBW	8.4	-	3.4:1
0.08	Smooth beam, 36°HPBW	8.0	-	11.2:1
0.1	Smooth beam, 36°HPBW	6.1	-	1.92:1
0.12	Smooth beam, 33°HPBW	6.2	-	5.04:1
0.14	Smooth beam, 28°HPBW	5.8	-	4.35:1
0.16	Wide beam, depressions at $\pm$36°	5.28	-	1.76:1
0.18	Wide beam, depressions at $\pm$37°	6.2	-	4.92:1
0.2	Wide beam, depressions at $\pm$38°	7.8	-	3.95:1
0.22	Wide beam, depressions at $\pm$40°	8.6	-	1.95:1
0.24	Wide beam, depressions at $\pm$45°	9.2	-	6.71:1
0.26	Wide beam, depressions at $\pm$47°	7.8	-	1.3:1
0.28	Wide beam, 72°HPBW	5.3	-	7.34:1
0.3	Wide beam, depressions at $\pm$39°	6.3	-	2.07:1

D.1.1.4 Pitch = 0.4λ

At 0.4λ acceptable patterns suitable for general use were found at radii of between 0.02λ and 0.16λ. More ripple and side lobes were present for pitches of 0.18λ to 0.3λ. All results can be seen in Table D.4.

Table D.4: Results for N=2, P=0.4 λ

Radius(λ)	**Shape of Pattern and Comments**	**Maximum Gain(dB)**	**Gain at centre if applicable(dB)**	**VSWR**
0.02	Smooth beam, 42°HPBW	8	-	45.3:1
0.04	Smooth beam, 47°HPBW	7.6	-	3.17:1
0.06	Smooth beam, 47°HPBW	7.2	-	8.99:1
0.08	Smooth beam, 49°HPBW	6.3	-	4.35:1
0.1	Smooth beam, 46°HPBW	5.9	-	3.12:1
0.12	Smooth beam, 42°HPBW	6.4	-	4.64:1
0.14	Smooth beam, 38°HPBW	6.41	-	2.5:1
0.16	Smooth beam, 37°HPBW	6.2	-	3.83:1
0.18	Smooth beam, 37°HPBW. Slight side lobes	6.55	-	4.54:1
0.2	Smooth beam, 38°HPBW. Slight side lobes	6.88	-	1.77:1
0.22	Smooth beam, 35°HPBW. Slight side lobes	6.9	-	4.34:1
0.24	Smooth beam, depression at 0°. Slight side lobes	6.27 at $\pm$28°	-	3.94:1
0.26	Smooth beam, depression at 0°. Slight side lobes	5.26 at $\pm$33°	-0.46	2.57:1
0.28	Smooth, flat beam. Side lobes present	5	-	5.17:1
0.3	Smooth, flat beam. Side lobes present	5.4	-	3.25:1

D.1.1.5 Pitch = 0.5λ

At 0.5λ good patterns for general use were found for radii between 0.02λ and 0.06λ. Patterns with depressions at 0° were noted between R=0.07λ and R=0.2λ. For radii greater than 0.2λ ripple and distorted patterns were noted. VSWR performance was generally less than 4:1 with some exceptions at R=0.02λ,0.04λ and 0.06λ. All results can be seen in Table D.5.

Table D.5: Results for N=2, P=0.5 λ

Radius(λ)	**Shape of Pattern and Comments**	**Maximum Gain(dB)**	**Gain at centre if applicable(dB)**	**VSWR**
0.02	Smooth beam, 58°HPBW	7.3	-	13.2:1
0.04	Smooth beam, 62°HPBW	6	-	11.2:1
0.06	Smooth beam, depression at 0°	5.3 at ±43°	4.2	6.31:1
0.08	Smooth beam, depression at 0°	5.01 at ±42°	1.64	2.3:1
0.1	Smooth beam, depression at 0°	5.2 at ±42°	-0.13	4.01:1
0.12	Smooth beam, depression at 0°	5.53 at ±39°	-0.36	3.55:1
0.14	Smooth beam, depression at 0°	5.27 at ±40°	-1.44	3.35:1
0.16	Smooth beam, depression at 0°	5.43 at±39°	-4.51	4.32:1
0.18	Smooth beam, depression at 0°	6.0 at ±40°	-7.5	2.75:1
0.2	Smooth beam, depression at 0°	6.2 at ±39°	-6.95	3.07:1
0.22	Smooth beam, decreasing towards 0°, increase in centre. Side lobes present	5.9	-	4.82:1
0.24	Smooth beam, decreasing towards 0°, increase in centre. Side lobes present	5.4	-	1.89:1
0.26	Smooth beam, decreasing towards 0°, increase in centre. Side lobes present	4.9	-	4.46:1
0.28	Smooth beam, decreasing towards 0°, increase in centre. Side lobes present	7.1	-	2.94:1
0.3	Slightly distorted beam	6.4	-	4.9:1

D.1.1.6 Pitch = 0.6λ

At P=0.6λ good general patterns were noted at for radii between 0.02λ and 0.06λ with a pattern with depression at 0° seen at R=0.06λ. For radii between 0.07λ and 0.3λ rippled and distorted patterns were seen. Results can be seen in Table D.6.

Table D.6: Results for N=2, P=0.6 λ

Radius(λ)	**Shape of Pattern and Comments**	**Maximum Gain(dB)**	**Gain at centre if applicable(dB)**	**VSWR**
0.02	Smooth beam	5.2	-	19.5
0.04	Smooth beam, depression at 0°	4.93 at ±53°	2.6	6.4:1
0.06	Smooth beam, depression at 0°	4.94 at ±53°	0.75	1.57:1
0.08	Wide beam. Depressions at ±26°	5.1	-	3.84:1
0.1	Wide beam. Depressions at ±36°	5.3	-	4.53:1
0.12	Very rippled beam	4.9	-	3.37:1
0.14	Very rippled beam	5.0	-	3.8:1
0.16	Multiple lobes	5.1	-	3.35:1
0.18	Multiple lobes	5.6	-	3.03:1
0.2	Multiple lobes	6.6	-	4.4:1
0.22	Multiple lobes	8.0	-	3.05:1
0.24	Multiple lobes	8.6	-	2.6:1
0.26	Multiple lobes	8.7	-	5.15:1
0.28	Multiple lobes	7.1	-	1.46:1
0.3	Wide, rippled beam	4.9	-	6.14:1

D.1.1.7 Pitch = 0.7λ

At P=0.7λ good patterns with depressions at 0° were found between 0.02λ and 0.04λ. All other patterns between 0.05λ and 0.3λ had either large ripple present or were distorted. All results can be seen in Table D.7.

Table D.7: Results for N=2, P=0.7 λ

Radius(λ)	**Shape of Pattern and Comments**	**Maximum Gain(dB)**	**Gain at centre if applicable(dB)**	**VSWR**
0.02	Smooth beam, depression at 0°	5.23 at ±61°	-6.13	5.16:1
0.03	Smooth beam, depression at 0°	5.34 at ±60°	-7.5	2.14:1
0.04	Smooth beam, depression at 0°	5.3 at ±60°	-8	2.39:1
0.05	Wide beam, depression at 0°. Slight ripple present	5.19 at ±60°	-7	3.93:1
0.06	Wide beam,decreasing towards 0°. Further depressions at ±36°	5.15	-5.6	5.39:1
0.07	Wide beam, depressions at ±38°	5.1	-	6.02:1
0.08	Wide beam, depressions at ±38°	4.9	-	5.58:1
0.1	Wide, rippled beam	5.2	-	3.32:1
0.12	Wide, rippled beam	5.8	-	3.22:1
0.14	Wide, rippled beam	5.7	-	3.73:1
0.16	Smooth beam with significant side lobes	5.4	-	3.44:1
0.18	Smooth beam with significant side lobes	5.4	-	3.95:1
0.2	Smooth beam with significant side lobes	6.1	-	3.47:1
0.22	Multiple lobes	6.6	-	2.6:1
0.24	Multiple lobes	6.6	-	4.33:1
0.26	Multiple lobes	6.0	-	3.22:1
0.28	Multiple lobes	5.2	-	2.7:1
0.3	Wide, rippled beam	6.2	-	5.25:1

D.1.1.8 Pitch = 0.8λ

At P=0.8λ no patterns were noted between 0.02λ and 0.3λ that did not either have a large amount of ripple or multiple, distorted beams present. Results can be seen in Table D.8.

Table D.8: Results for N=2, P=0.8 λ

Radius(λ)	**Shape of Pattern and Comments**	**Maximum Gain(dB)**	**Gain at centre if applicable(dB)**	**VSWR**
0.02	Multiple lobes	6	-	16.3:1
0.04	Multiple lobes	5.5	-	10.8:1
0.06	Wide, very rippled beam	6.0	-	6.34:1
0.08	Wide, very rippled beam	6.6	-	2.58:1
0.1	Wide, very rippled beam	6.9	-	3.0:1
0.12	Wide, very rippled beam	6.8	-	4.26:1
0.14	Wide, very rippled beam	6.5	-	3.87:1
0.16	Wide, very rippled beam			3.62:1
0.18	Multiple lobes	6.2	-	3.54:1
0.2	Multiple lobes	6.0	-	3.07:1
0.22	Multiple lobes	6.1	-	3.82:1
0.24	Multiple lobes	5.5	-	3.91:1
0.26	Multiple lobes	6.7	-	2.23:1
0.28	Multiple lobes	8.4	-	4.64:1
0.3	Multiple lobes	8.8	-	2.72:1

D.1.2 Results for N = 3 Turns

D.1.2.1 Pitch= 0.1 λ

Good radiation patterns (suitable for general use) were found at P=0.1λ for R>0.04λ. VSWR was very varied with a maximum 639:1 at R=0.06λ and minimum of 2.03:1 at R=0.14λ. All results can be seen in Table D.9.

Table D.9: Results for N=3, P=0.1 λ

Radius(λ)	**Shape of Pattern and Comments**	**Maximum Gain(dB)**	**Gain at centre if applicable(dB)**	**VSWR**
0.02	Very Narrow beam	-10.4	-	107:1
0.06	"indented" beam	2.4	-	640:1
0.08	Wide beam	-0.4	-	15.1:1
0.1	Normal beam,26°HPBW, slight side lobes	2.28	-	25:1
0.12	Wide beam, 43°HPBW	6.8	-	12.2:1
0.14	Wide beam, 56°HPBW	7	-	2.03:1
0.16	Wide beam, 58°HPBW	6.74	-	5.78:1
0.18	Wide beam, 60°HPBW	6.5	-	2.92:1
0.2	Wide beam, 60°HPBW	6.4	-	8.97:1
0.22	Wide beam, 43°HPBW	8.17	-	20.9:1
0.24	Wide beam, 51°HPBW	7.3	-	16:1
0.26	Wide beam, 57°HPBW	6.48	2.31	2.3:1
0.28	Wide beam,36°HPBW	9.2	-	24:1
0.3	Wide beam, 58°HPBW	6.18	-	67.9:1

D.1.2.2 Pitch= 0.2 λ

At P=0.2λ good radiation patterns with generally narrow beams were found for R>0.04λ.No cardiod patterns were found in this region. VSWR performance was generally acceptable for R>0.1λ. All results can be seen in Table D.10.

Table D.10: Results for N=3, P=0.2 λ

Radius(λ)	**Shape of Pattern and Comments**	**Maximum Gain(dB)**	**Gain at centre if applicable(dB)**	**VSWR**
0.04	Smooth, wide beam, 47°HPBW	2.64	-	20.8:1
0.06	Wide beam, 37°HPBW	0.32	-	227:1
0.08	Wide beam, slight sidelobes, 30°HPBW	9.95	-	55.2:1
0.1	Wide beam, 31°HPBW	9.08	-	2.86:1
0.12	Wide beam, 28°HPBW	7.9	-	2.36:1
0.14	Wide beam, depressions at $\pm$40°	7.86	-	4.55:1
0.16	Wide beam, depressions at $\pm$42°	7.8	-	1.51:1
0.18	Wide beam, depressions at $\pm$42°	8.7	-	5.11:1
0.2	Wide beam, depressions at $\pm$44°	9.7	-	1.19:1
0.22	Wide, “dummy-shaped” beam	9.2	-	5.35:1
0.24	Wide beam, “dummy-shaped” beam	6.6	-	7.33:1
0.26	Wide beam, “dummy-shaped” beam	8.5	-	4.01:1
0.28	Wide beam, “dummy-shaped” beam	7.57	-	2.48:1
0.3	Wide beam,“dummy-shaped” beam	6.56	-	10.5:1

D.1.2.3 Pitch= 0.3 λ

At P=0.3λ good, narrow beams suitable for general use were found for R=0.05λ to R=0.1λ. For R=0.11λ to R=0.2λ radiation patterns with a depression at 0°were found. These patterns, however, had relatively low beam widths. For R>0.22λ more rippled patterns were found. VSWR was generally below 5:1 for R>0.06λ. All results can be found in Table D.11.

Table D.11: Results for N=3, P=0.3 λ

Radius(λ)	**Shape of Pattern and Comments**	**Maximum Gain(dB)**	**Gain at centre if applicable(dB)**	**VSWR**
0.01	Wide, flat beam, depression at 0°	0.72	-4.6	159:1
0.02	Wide beam, depressions at 0°	14.5 at 55°	3.77	1048:1
0.05	Smooth beam, 27°HPBW	10.4	-	38.5:1
0.06	Smooth beam, 29°HPBW	10.2	-	4.67:1
0.08	Wide beam, 48°HPBW	7.1	-	4.73:1
0.1	Wide beam, 50°HPBW	5.87	-	3.54:1
0.12	Wide beam, depression at 0°	5.89 at ±37°	4.24	3.71:1
0.13	Wide beam, depression at 0°	6.14 at ±36°	3.8	3.43:1
0.14	Wide beam, depression at 0°	6.35 at ±33°	3.7	2.62:1
0.15	Wide beam, depression at 0°	6.12 at ±37°	3.37	2.76:1
0.16	Wide beam, depression at 0°	6.24 at ±36°	2.49	3.99:1
0.17	Wide beam, depression at 0°	6.45 at ±34°	1.38	3.91:1
0.18	Wide beam, depression at 0°	6.59 at ±34°	0.6	2.21:1
0.19	Wide beam, depression at 0°	6.72 at ±35°	-10.12	2.24:1
0.2	Wide beam, depression at 0°, significant side lobes	6.66 at ±36°	-1.54	4.48:1
0.21	Wide beam, depression at 0°, significant side lobes	6.34 at ±37°	-3.31	4.21:1
0.22	Wide beam, depression at 0°, significant ripple	5.98 at ±37°	-3.31	4.21:1
0.23	Wide beam, depression at 0°, significant ripple	5.5 at ±38°	1.3	3.9:1
0.24	Wide, rippled beam	5.1	-	6.12:1
0.26	Wide beam, 45°HPBW, side lobes present	6.13	-	5.75:1
0.28	Wide, flat beam. Depression at 0°	5.57 at ±40°	0.91	1.82:1
0.3	Wide, rippled beam	6.2	-	3.09:1

D.1.2.4 Pitch= 0.4 λ

For P = 0.4λ good general use radiation patterns were found for R=0.02λ to R=0.08λ. For R $>$ 0.1λ the radiation pattern was quite rippled. The VSWR was generally below 5:1. All results can be seen in Table D.12.

Table D.12: Results for N=3, P=0.4 λ

Radius(λ)	**Shape of Pattern and Comments**	**Maximum Gain(dB)**	**Gain at centre if applicable(dB)**	**VSWR**
0.02	Smooth beam	12.3	-	113:1
0.04	Wide beam,38°HPBW. Side lobes present	9.59	-	2.73:1
0.06	Tall, wide beam. 42°HPBW	8.12	-	6.48:1
0.08	Tall, wide beam. 60°HPBW	6.19	-	2.77:1
0.1	Wide, rippled beam	6.08	-	4.33:1
0.12	Wide beam, depressions at $\pm$34°. Significant side lobes	5.6	-	2.94:1
0.14	Wide beam, depressions at $\pm$34°. Significant side lobes	5.9	-	4.03:1
0.16	Wide beam, depressions at $\pm$33°. Significant side lobes	6.9	-	2.96:1
0.18	Multiple lobes	7.3	-	3.59:1
0.2	Multiple lobes	8.4	-	3.21:1
0.22	Multiple lobes	8.5	-	3.91:1
0.24	Multiple lobes	7	-	2.33:1
0.26	Wide beam, significant ripple	5.3	-	6.76:1
0.28	Wide beam, significant ripple	6.3	-	3.52:1
0.3	“dummy” shaped	5.62	-	1.11:1

D.1.2.5 Pitch= 0.5 λ

For P = 0.5λ good general radiation patterns were found for R=0.02λ. Patterns with depressions at 0°were found for R=0.04λ to R=0.18λ. For R $>$ 0.1 however some ripple was present at the side of the beam. For R $>$ 0.2 the radiation patterns were very rippled or distorted. VSWR was generally below 5:1 for R $>$ 0.04λ. All results can be seen in TableD.13.

Table D.13: Results for N=3, P=0.5 λ

Radius(λ)	**Shape of Pattern and Comments**	**Maximum Gain(dB)**	**Gain at centre if applicable(dB)**	**VSWR**
0.02	Wide beam, 48°HPBW	8.1	-	10.8:1
0.04	Wide beam,depression at 0°	6.63 at ±37°	5.59	7.12:1
0.05	Wide beam,depression at 0°	6.12 at ±36°	3.99	3.63:1
0.06	Wide beam,depression at 0°	5.65 at ±38°	2.25	2.22:1
0.07	Wide, flat beam. Depression at 0°	5.33 at ±37°	0.69	3.31:1
0.08	Wide, flat beam. Depression at 0°	5.24 at ±36°	-0.04	4.18:1
0.09	Wide, flat beam. Depression at 0°	5.17 at ±35°	-0.01	3.74:1
0.1	Wide, flat beam. Depression at 0°	4.99 at ±33°	0.18	3.15:1
0.11	Wide, flat beam. Depression at 0°. Slight ripple at sides of lobe	4.63 at ±32°	-0.2	3.48:1
0.12	Wide, flat beam. Depression at 0°. Slight ripple at sides of lobe	4.66 at ±31°	-1.22	4.03:1
0.14	Wide beam, depression at 0°. Ripple present in side lobes	5.6 at ±33°	-3.57	3.25:1
0.16	Wide, flat beam. Depression at 0°. Ripple present in sides lobes	5.9 at ±33°	-3.83	3.51:1
0.18	Wide, flat beam. Depression at 0°. Ripple present in sides lobes	6.1 at ±33°	-7.5	3.85:1
0.2	Multiple lobes	6.63 at ±34°	-7.26	2.64:1
0.22	Wide beam. Large ripple	6.0	-	4.67:1
0.24	Wide beam. Large ripple	3.1	-	2.6:1
0.26	Wide beam. Large ripple	7.3	-	4.11:1
0.28	Wide beam. Large ripple	5.6	-	6.03:1
0.3	Wide beam. Large ripple	5.6	-	2.37:1

D.1.2.6 Pitch= 0.6 λ

For P=0.6λ patterns with depressions at 0°were found for R=0.01λ to R=0.06λ. For R $>$ 0.08λ patterns had a large amount of ripple. VSWR was below 5:1 for R= 0.03λ to R=0.27λ. All results can be seen in Table D.14.

Table D.14: Results for N=3, P=0.6 λ

Radius(λ)	**Shape of Pattern and Comments**	**Maximum Gain(dB)**	**Gain at centre if applicable(dB)**	**VSWR**
0.01	Wide, smooth beam with depression at 0°	6.2 at ±50°	1.58	13.5:1
0.02	Wide, smooth beam with depression at 0°	6.18 at ±50°	0.01	5.52:1
0.03	Wide, smooth beam with depression at 0°	6.19 at ±50°	-1.69	1.74:1
0.04	Wide, smooth beam with depression at 0°	6.08 at ±52°	-2.7	1.86:1
0.05	Wide beam, decreasing towards centre but slight increase at 0°	5.78 at ±52°	-1.48	3.76:1
0.06	Wide beam, decreasing towards centre but slight increase at 0°	5.4 at ±50°	-1.52	4.77:1
0.08	Wide, rippled beam	5.1	-	3.23:1
0.1	Wide, rippled beam	5.5	-	3.78:1
0.12	Wide, rippled beam	5.1	-	3.43:1
0.14	Wide, rippled beam	4.9	-	6.68:1
0.16	Wide, rippled beam	6.1	-	3.84:1
0.18	Wide, rippled beam	6.6	-	2.84:1
0.2	Wide, rippled beam	6.9	-	4.56:1
0.22	Wide, rippled beam	7.6	-	2.06:1
0.24	Wide, rippled beam	7.0	-	5.48:1
0.26	Wide, rippled beam	5.4	-	1.56:1
0.28	Wide, rippled beam	5.9	-	5.53:1
0.3	Wide, rippled beam	6.2	-	5.34:1

D.1.2.7 Pitch= 0.7 λ

All radiation patterns for P=0.7 either had multiple lobes or were very rippled. VSWR was generally below 5:1 for R=0.04λ to R=0.29λ. All results can be seen in Table D.15.

Table D.15: Results for N=3, P=0.7 λ

Radius(λ)	**Shape of Pattern and Comments**	**Maximum Gain(dB)**	**Gain at centre if applicable(dB)**	**VSWR**
0.01	Multiple lobes	7.2	-	17.9:1
0.02	Multiple lobes	6.8	-	11.4:1
0.04	Wide beam, multiple depressions	6.4	-	6.2:1
0.06	Wide, rippled beam	6.2	-	2.22:1
0.08	Wide, rippled beam	5.9	-	3.4:1
0.1	Wide, rippled beam		-	3.71:1
0.12	Wide, rippled beam	6.3	-	3.64:1
0.14	Wide, rippled beam	6.1	-	3.73:1
0.16	Wide, rippled beam	5.8	-	3.24:1
0.18	Wide, rippled beam	6.1	-	4.24:1
0.2	Wide, rippled beam with deep depressions	6	-	2.66:1
0.22	Wide, rippled beam with deep depressions	6	-	4.46:1
0.24	Wide, rippled beam with deep depressions	7.8	-	2.56:1
0.26	Wide, rippled beam	8.8	-	5.4:1
0.28	Wide, rippled beam	8.2	-	1.49:1
0.3	Wide, rippled beam	6.2	-	6.17:1

D.1.2.8 Pitch= 0.8 λ

All radiation patterns for P=0.8 were very rippled.. VSWR was generally below 6:1. All results can be seen in Table D.16.

Table D.16: Results for N=3, P=0.8 λ

Radius(λ)	**Shape of Pattern and Comments**	**Maximum Gain(dB)**	**Gain at centre if applicable(dB)**	**VSWR**
0.02	Multiple lobes	7.2	-	3.34:1
0.04	Rippled beam	7.0	-	3.34:1
0.06	Rippled beam	6.8	-	5.3:1
0.08	Rippled beam	7.3	-	3.44:1
0.1	Rippled beam	7.7	-	3.37:1
0.12	Rippled beam	7.4	-	3.8:1
0.14	Rippled beam	6.9	-	3.53:1
0.16	Rippled beam	6.8	-	3.98:1
0.18	Rippled beam	6.2	-	3.07:1
0.2	Rippled beam	6.1	-	4.09:1
0.22	Rippled beam	6.9	-	3.22:1
0.24	Rippled beam	7.2	-	3.64:1
0.26	Rippled beam	5.9	-	3.82:1
0.28	Rippled beam	6.1	-	4.78:1
0.3	Rippled beam	6.6	-	1.77:1

D.1.3 Results for N = 4 Turns

D.1.3.1 General

This number of turns gave quite acceptable performance for pitches ranging from 0.2λ to 0.6λ. For pitches of 0.7λ to 1λ radiation patterns with a high amount of ripple and distorted patterns were noted.

D.1.3.2 Pitch = 0.1λ

For P=0.1λ most radiation patterns from R=0.05λ to 0.3λ had narrow beams with good general performance. The VSWR,however, of a lot of antennas was unacceptably high. R = 0.14λ and R=0.17λ had good VSWR performance. All results can be seen in Table D.17.

Table D.17: Results for N=4, P=0.1λ

Radius(λ)	**Shape of Pattern and Comments**	**Maximum Gain(dB)**	**Gain at centre if applicable(dB)**	**VSWR**
0.05	Narrow beam	-6.5	-	186
0.06	Wide beam with depression at 0°	-6	-12	19.3:1
0.07	Narrow beam	-5.4	-	52.3:1
0.08	Narrow beam	2.1	-	19.9:1
0.09	Wide beam	-1.5	-	46:1
0.11	Narrow beam	8.6	-	47.6:1
0.12	Narrow beam	9	-	4.53:1
0.13	Narrow beam	7	-	8.17:1
0.14	Narrow beam	6.3	-	1.55:1
0.15	Narrow beam	5.4	-	5:1
0.16	Narrow beam	5.6	-	6.51:1
0.17	Narrow beam	5.3	-	1.39:1
0.18	Narrow beam	5.6	-	8.07:1
0.19	Wider beam with slight ripple	6.18	-	6.98:1
0.21	Narrow beam	9.0	-	10.2:1
0.22	Narrow beam	6.8	-	10.3:1
0.23	Narrow beam	6.34	-	14.1:1
0.24	Narrow beam	7.9	-	20.4:1
0.25	Narrow beam	9.0	-	15.3:1
0.26	Narrow beam	6.3	-	28.4:1
0.27	Narrow beam	6.4	-	19.1:1
0.28	Narrow beam	7.97	-	44.7:1
0.29	Narrow beam	8.8	-	18.1:1

D.1.3.3 Pitch = 0.2λ

This region gave a relatively good performance in terms of radiation patterns and gain. A good general pattern with maximum at 0°was noted for radii of 0.09λ to 0.14λ with gains of 9.5dB down to 7.3dB. For R=0.14λ to 0.29λ (with noted exceptions at 0.23$\lambda$and 0.27λ) a small depression at 0°was noted with the maximum gain being at the rim of the pattern. In terms of VSWR, performance was varied with the best VSWR of 1.05:1 noted at 0.22λ and the worst of 604:1 at 0.06λ. All results are presented in Table D.18.

Table D.18: Results for N=4, P=0.2λ

Radius(λ)	**Shape of Pattern and Comments**	**Maximum Gain(dB)**	**Gain at centre if applicable(dB)**	**VSWR**
0.05	Narrow beam with slight side lobes	4	-	22.3:1
0.06	Wide beam	11.2	-	604
0.07	Wide beam, slight depression at 0°	3.59	1.87	8.78:1
0.08	Wide beam with increase (“notch) at centre	6.34	-	6.34:1
0.09	Wide beam	9.5	-	1.61:1
0.1	Wide beam	8.24	-	5.84:1
0.11	Wide beam	7.58	-	2.91:1
0.12	Wide beam	7.5	-	2.42:1
0.13	Wide beam	7.3	-	3.28:1
0.14	Wide beam with depression at 0°	7.3	6.9 4	3.52:1
0.15	Wide beam with depression at 0°	7.4	7.01	1.98:1
0.16	Wide beam with depression at 0°	7.3	6.7	2.91:1
0.17	Wide beam with depression at 0°	7.3	6.2	4.17:1
0.18	Wide beam with depression at 0°	7.34	5.81	1.87:1
0.19	Wide beam with depression at 0°	7.3	5.03	3.14:1
0.2	Wide beam with depression at 0°	6.9	3.1	4.99:1
0.21	Wide beam with depression at 0°	6.3	1.5	1.05:1
0.22	Wide beam with depression at 0°	5.73	4.14	6.64:1
0.23	Wide beam	7.06	-	2.14:1
0.24	Wide beam	7.3	-	7.74:1
0.25	Narrower beam with depression at 0°	6.56	3.93	2.09:1
0.26	Narrower beam with depression at 0°	5.6	5.06	9.82:1
0.27	Narrower beam	7.37	-	2.29:1
0.28	Narrower beam with slight depression at 0°	6.8	6.1	12.4:1
0.29	Narrower beam with depression at 0°	5.8	3.4	1.93:1
0.3	Narrower beam	5.26	-	12.4:1

D.1.3.4 Pitch = 0.3λ

For P=0.3λ many more radiation patterns presented side lobes. Acceptable beams with good, general performance were found at R=0.06λ to 0.08λ. For R=0.09 to 0.3 all patterns included side beams or were distorted. VSWR was generally lower for all antennas. All results can be seen in Table D.19.

Table D.19: Results for N=4, P=0.3λ

Radius(λ)	**Shape of Pattern and Comments**	**Maximum Gain(dB)**	**Gain at centre if applicable(dB)**	**VSWR**
0.05	Very wide beam with increased gain as "notch" in centre	6.76	-	13.7:1
0.06	Narrow beam, Small sidelobes	11.5	-	7.15:1
0.07	Narrow beam	10	-	7.83:1
0.08	Narrow beam	8.9	-	2.6:1
0.09	Narrow beam with side lobes	8.5	-	4.11:1
0.1	Very wide beam with depressions at $\pm 39^\circ$	7.74	-	3.1:1
0.11	Very wide beam with depressions at $\pm 35^\circ$	7.3	-	3.48:1
0.12	Distorted wide beam (multiple side lobes)	7.52	-	4.08:1
0.13	Distorted wide beam (multiple side lobes)	7.5	-	2.8:1
0.14	Distorted, narrower beam (multiple side lobes)	7.26	-	2.91:1
0.15	Distorted, narrower beam (multiple side lobes	7.7	-	4.27:1
0.16	Distorted, narrower beam (multiple side lobes	8.1	-	3.05:1
0.17	Distorted, narrower beam (multiple side lobes	8.3	-	2.12:1
0.18	Distorted, narrower beam (multiple side lobes	8.4	-	4.43:1
0.19	Distorted, narrower beam (multiple side lobes)	8.72	-	3.56:1
0.2	Distorted, narrower beam (multiple side lobes	8.72	-	1.61:1
0.21	Wide beam with side lobes	8.1	-	5.26:1
0.22	Distorted, wide beam with side lobes	7	-	3.2:1
0.23	Distorted, wide beam with side lobes	5.8 at $\pm$ 23°	4.3	3.02:1
0.24	Distorted, wide beam with side lobes	6 at $\pm$ 51°	4.07	5.52:1
0.25	Distorted, narrower beam with side lobes	6.41	-	2.05:1
0.26	Distorted, narrower beam with side lobes	7.4	-	6.38:1
0.27	rippled, distorted, wide beam	6.34 at $\pm$ 23°	5.6	2.51:1
0.28	Rippled, distorted, wide beam	5.2 at $\pm$ 51°	4.79	7.25:1
0.3	Wide beam with nulls at $\pm 43^\circ$	6.2	-	5.71:1

D.1.3.5 Pitch = 0.4λ

For P=0.4λ good general patterns were found at R=0.05λ to 0.08λ. At R=0.09λ to 0.11λ patterns with depressions at 0°were found. For R>0.13λ patterns with high side lobes, ripple and distorted beams were found. The VSWR was below 4:1 for most of the region. All results can be seen in Table D.20.

Table D.20: Results for N=4, P=0.4λ

Radius(λ)	**Shape of Pattern and Comments**	**Maximum Gain(dB)**	**Gain at centre if applicable(dB)**	**VSWR**
0.05	Wide beam	9.8	-	6.84:1
0.06	Narrower beam	7.9	-	3.71:1
0.08	Wider beam with slight decrease at 0°	6.27	5.46	3.9:1
0.09	Wider beam with slight decrease at 0°	5.95	4.86	3.79:1
0.1	Wider beam with slight decrease at 0°	6.07	3.9	3.55:1
0.11	Wider beam with slight increase at 0°,more ripple	6.12	2.86	3.33:1
0.12	Wide, rippled beam	6.3	-	3.38:1
0.13	Wide, rippled beam	6.05	3.36	3.96:1
0.14	Wide, rippled beam	6.2	-	3.52:1
0.15	Wide, rippled beam	6.56	3.02	2.67:1
0.16	Wide, rippled beam	6.6	-	3.69:1
0.17	Wide, rippled beam	6.25	5.11	4.19:1
0.18	Wide, rippled beam	6.3	-	2.37:1
0.19	Wide, rippled beam	6.36	-	3.05:1
0.2	Wide, rippled beam	7.6	-	4.92:1
0.21	Distorted, rippled beam	8.56	-	2.35:1
0.23	Distorted, rippled beam	8.73	-	5.58:1
0.24	Distorted, rippled beam	6.3	-	2.43:1
0.25	Wide, rippled beam	5.18	-	5.55:1
0.26	Wide, rippled beam	6.3	-	2.43:1
0.27	Wide, rippled beam	6	-	5.39:1
0.28	Wide, rippled beam	7.3	-	3.28:1
0.29	Wide, rippled beam	5.47	-	5.18:1
0.3	Wide, rippled beam	5.8	-	3.12:1

D.1.3.6 Pitch = 0.5λ

At P=0.5λ good performance was found at R=0.02λ to R=0.06λ. All other patterns were either very rippled or distorted. VSWR performance was generally good and below 5:1 for most antennas. All results can be seen in Table D.21.

Table D.21: Results for N=4, P=0.5λ

Radius(λ)	**Shape of Pattern and Comments**	**Maximum Gain(dB)**	**Gain at centre if applicable(dB)**	**VSWR**
0.02	Wide beam	8.4	-	9.5:1
0.04	Wide beam with depression at centre	6.9	4.6	3.37:1
0.05	Wide beam with depression at centre	6.25 at 35°BW	2.39	2.19:1
0.06	Wide beam with depression at centre	5.63 at 36°BW	0.73	3.6:1
0.07	Wide beam with depression at centre and some ripple	5.09 at 32°BW	0.14	3.57:1
0.08	Wide beam with depression at centre and some ripple	4.66 at 31°BW	0.41	3.24:1
0.1	Wide beam with depression at centre and some ripple	4.21	0.02	3.85:1
0.12	Very rippled beam with depression at centre	5.17 at $\pm$ 30°	-1.192	3.41:1
0.13	Very rippled beam with depression at centre	5.53 at $\pm$ 30°	-1.64	3.29:1
0.14	Very rippled beam with depression at centre	5.23 at $\pm$ 30°	-2.52	3.76:1
0.15	Very rippled beam with depression at centre	5.59 at $\pm$ 30°	-15.12	3.92:1
0.16	Very rippled beam with depression at centre	6.3 at $\pm$ 30°	-7.6	3.03:1
0.17	Very rippled beam with depression at centre	6.53 at $\pm$ 30°	-8	2.99:1
0.18	Very rippled beam with large depression at centre	6.5 at $\pm$ 30°	-7.3	4.25:1
0.2	Very rippled beam	6.6	-3.3	2.18:1
0.22	Very rippled beam	5.38	3.5	4.31:1
0.24	Very rippled beam	6.77	-	4.99:1
0.26	Very rippled beam	6.62	-	2.73:1
0.28	Very rippled beam	5.93 at $\pm$ 31°	0.93	1.65:1
0.3	Multiple lobes	6.73	-	1.23:1

D.1.3.7 Pitch = 0.6λ

For P= 0.6λ useful patterns with depressions at 0°were found for R=0.02λ to R=0.04λ. All other patterns showed a high amount of ripple or distortion. VSWR performance was generally below 4:1 with a few exceptions. All results can be seen in Table D.22.

Table D.22: Results for N=4, P=0.6λ

Radius(λ)	**Shape of Pattern and Comments**	**Maximum Gain(dB)**	**Gain at centre if applicable(dB)**	**VSWR**
0.02	Wide beam with depression at 0°	7.3	-9	2.41:1
0.03	Wide beam with slight depression at 0°	7.08 at ±52°	-6.5	3.82:1
0.04	Wide beam with large area of depression between +29° to −29°	6.5 ±52°	-3.7	4.97:1
0.05	Wide rippled beam	6.56 at ±60°	-2.37	3.97:1
0.06	Wide very rippled beam	6.07 at ±60°	-1.67	2.99:1
0.08	Wide very rippled beam	5.69 at ± 60°	0.32	3.78:1
0.1	Wide very rippled beam	5	-	3.37:1
0.12	Very rippled beam	5.2	-	3.88:1
0.14	Very rippled beam	5.28 at ±20°	3.14	3.27:1
0.18	Very rippled beam	6.7 at ±20°	3.08	2.78:1
0.2	Very rippled beam	6.5 at ±23°	0.77	4.35:1
0.22	Very rippled beam	6.96 at ±24°	-2.1	2.84:1
0.24	Very rippled beam	4.9	-	2.79:1
0.26	Wide, very rippled beam	6.27 at ±42°	2.5	5.79:1
0.28	Distorted, rippled beam	5.3	-	6.14:1
0.3	Distorted, rippled beam	6	-	6.01:1

D.1.3.8 Pitch = 0.7λ

No useful radiation patterns were found for P = 0.7λ. All patterns displayed a large amount of ripple. VSWR for most antennas was below 5:1. All results can be seen in Table D.23.

Table D.23: Results for N=4, P=0.7λ

Radius(λ)	**Shape of Pattern and Comments**	**Maximum Gain(dB)**	**Gain at centre if applicable(dB)**	**VSWR**
0.01	Wide beam with large depressions at $\pm 40^\circ$	7.56 at $\pm 65^\circ$	-3	10.4:1
0.02	Wide beam with depressions at $\pm 42^\circ$	7.6 at $\pm 67^\circ$	-4.2	3.94:1
0.03	Wide beam with depressions at $\pm 43^\circ$	7.65 at $\pm 67^\circ$	-5.3	1.14:1
0.04	Wide, rippled beam	7.11	-5.7	2.52:1
0.06	Wide, rippled beam	6.6	-	4.17:1
0.08	Wide, rippled beam	6.1	-	3.17:1
0.1	Wide, rippled beam	6.0	-	3.74:1
0.12	Wide, rippled beam	6.3	-	3.52:1
0.14	Wide, rippled beam	6.1	-	3.85:1
0.16	Wide, rippled beam	6.2	-	3.26:1
0.18	Rippled, distorted beam	6.6	-	4.02:1
0.2	Rippled, distorted beam	7.6	-	2.95:1
0.22	Rippled, distorted beam	7.8	-	3.82:1
0.24	Rippled, distorted beam	7.6	-	4.21:1
0.26	Rippled, distorted beam	5.4	-	1.72:1
0.28	Rippled, distorted beam		-	3.39:1
0.3	Rippled, distorted beam	6.5	-	6.09:1

D.1.3.9 Pitch = 0.8λ

No useful radiation patterns were found for P = 0.8λ. All patterns displayed a large amount of ripple or multiple lobes. VSWR for most antennas was below 4:1. All results can be seen in Table D.24.

Table D.24: Results for N=4, P=0.8λ

Radius(λ)	**Shape of Pattern and Comments**	**Maximum Gain(dB)**	**Gain at centre if applicable(dB)**	**VSWR**
0.04	Wide, rippled beam	7.9		1.98:1
0.06	Wide, rippled beam	7.3	-	3.47:1
0.08	Wide, rippled beam	7.6	-	3.68:1
0.1	Wide, rippled beam	8.2	-	3.56:1
0.12	Wide, rippled beam	7.7	-	3.62:1
0.14	Wide, rippled beam	7.3	-	3.68:1
0.16	Wide, rippled beam	7	-	3.69:1
0.18	Wide, rippled beam	6.3	-	3.45:1
0.2	Wide, rippled beam	7.6	-	3.69:1
0.22	Wide, rippled beam	8.4	-	3.6:1
0.24	Wide, rippled beam	9.7	-	2.73:1
0.26	Wide, rippled beam	9	-	5.39:1
0.28	Wide, rippled beam	5.5	-	3.83:1
0.3	Wide, rippled beam	6	-	2.06:1

D.1.4 Results for N = 5 Turns

D.1.4.1 P= 0.1 λ

For P=0.1 a wide beam with central depression was noted at R=0.08λ. The VSWR for this antenna was, however, unacceptably high. Good general performance was noted from R=0.07λ to 0.3λ. The VSWR for most antennas was very high however. Better VSWR performance was noted at R=0.22λ and R=0.14λ. All results can be seen in Table D.25.

Table D.25: Results for N=5, P=0.1 λ

Radius(λ)	**Shape of Pattern and Comments**	**Maximum Gain(dB)**	**Gain at centre if applicable(dB)**	**VSWR**
0.06	Narrow beam	-2.8	-	18.8:1
0.07	Narrow beam	-0.9	-	77.7:1
0.08	Wide beam, depression at 0 °	-3.34	-18	19:1
0.09	Wide beam	4.9	-	30.8:1
0.1	Round, pointed beam. 31° HPBW	6.15	-	32.9:1
0.12	Round, pointed beam. 27° HPBW	10.7	-	8.46:1
0.14	Round, pointed beam. 27° HPBW	8.7	-	2.33:1
0.16	Round, pointed beam. 26° HPBW	8.5	-	4.28:1
0.18	Round, pointed beam. 24° HPBW	9.7	-	7.56:1
0.20	Round, pointed beam. 29° HPBW	9.8	-	8.16:1
0.22	Round, pointed beam. 28° HPBW	8.6	-	1.21:1
0.24	Wide beam	6.9	-	19.7:1
0.26	Wide beam	9.1	-	43.3:1
0.28	Wide beam	7.9	-	16.9:1
0.3	Wide beam	7.3	-	8.37:1

D.1.4.2 P=0.2 λ

For P=0.2λ there were some wide beams noted at R=0.08λ, 0.12λ-0.18λ, and 0.22λ. Good general patterns were found at other radii between 0.07λ and 0.3λ. VSWR was below 5:1 between R=0.1λ and R=0.22λ. All results can seen in Table D.26.

Table D.26: Results for N=5, P=0.2 λ

Radius(λ)	**Shape of Pattern and Comments**	**Maximum Gain(dB)**	**Gain at centre if applicable(dB)**	**VSWR**
0.07	Normal beam with slight side lobes	7.8	-	9.9:1
0.08	Wide beam, depression at 0°	4.18 at ±51°	2.03	74.5:1
0.09	Narrow beam 23°HPBW	11.7	-	11.2:1
0.1	Wide beam 30°HPBW	9.01	-	2.18:1
0.12	Wide beam 54°HPBW	6.01	-	2.25:1
0.14	Wide beam with depression at 0°	6.34	4.5	3.2:1
0.16	Rippled beam with side lobes	6.6	4.7	4.32:1
0.18	Rippled beam with side lobes	6.5	6.07	3.67:1
0.2	Distorted beam	8.6	-	2.49:1
0.22	Wide, rippled, beam 50°HPBW with side lobes	7.38	-	3.18:1
0.24	Wide, rippled, beam 28°HPBW with side lobes	7.7	-	8.05:1
0.26	Wide beam with depressions at ±24°	6.42	5.27	7.25:1
0.28	Wide beam	7.8	-	2.0:1
0.3	Wide beam	6.6	-	6.61:1

D.1.4.3 P= 0.3 λ

For P = 0.3λ the following was noted. Between R=0.04λ and R=0.08λ good general patterns were found. Between R=0.1λ and R=0.17λ wider patterns with a depression at 0°were found. Some ripple was noted on the side of these patterns. For R>0.18λ more ripple on the main beam was seen. VSWR performance was below 5:1 for most antennas. All results can be seen in Table D.27.

Table D.27: Results for N=5, P=0.3 λ

Radius(λ)	**Shape of Pattern and Comments**	**Maximum Gain(dB)**	**Gain at centre if applicable(dB)**	**VSWR**
0.04	Normal beam 32°HPBW	10.9	-	49.4:1
0.06	Narrow beam, 19°HPBW	12.9	-	13.6:1
0.08	Wide beam, 40°HPBW	8.8	-	3.76:1
0.09	Wide beam, 16°HPBW	6.7	-	3.79:1
0.1	Wide beam, depression at 0°	6.6	5.3	3.1:1
0.11	Wide beam, depression at 0°	6.5 at ±36°	4.37	3.72:1
0.12	Wide beam, depression at 0°	6.66 at ±36°	2.74	3.55:1
0.13	Wide beam, depression at 0°	6.8 at ±36°	1.7	2.71:1
0.14	Wide beam, depression at 0°	6.78 at ±34°	1.31	3.91:1
0.15	Wide rippled beam, depressions at ±14° but still less at 0°	6.98 at ±35°	0.1	3.14:1
0.16	Wide, rippled, beam, depressions at ±13° but still less at 0°	7.2 at ±35°	0.02	2.53:1
0.17	Wide, rippled, beam, depressions at ±15° but still less at 0°, side lobes present	6.98 at ±36°	1.57	4.44:1
0.18	Wide, rippled, beam, depressions at ±16° but still less at 0°, side lobes present	6.8 at ±35°	2.5	2.05:1
0.2	Very rippled beam	6.5	-	3.86:1
0.22	Very rippled beam	8.07	-	5.3:1
0.24	Wide,rippled beam	6.72 at ±36°	3.8	4.79:1
0.26	Wide, rippled beam	7.5	-	2.05:1
0.28	Wide,rippled beam	5.8	-	3.43:1
0.3	Wide,rippled beam	5.06	-	6.44:1

D.1.4.4 P= 0.4 λ

For P = 0.4λ good general performance was noted between R = 0.04λ and R=0.08λ. For R=0.1λ to R=0.16λ beams with depressions at 0°were found. These patterns, however, had a large amount of ripple.For all patterns for R>0.18λ very rippled beams were found. The VSWR was below 5:1 for R<0.28λ. All results can be seen in Table D.28.

Table D.28: Results for N=5, P=0.4 λ

Radius(λ)	**Shape of Pattern and Comments**	**Maximum Gain(dB)**	**Gain at centre if applicable(dB)**	**VSWR**
0.04	Narrow beam, 26°HPBW	12.1	-	3.63:1
0.06	Wider beam, 45°HPBW	7.4	-	2.76:1
0.07	Wide beam, depression at 0°	6.7 at ±36°	5.8	3.59:1
0.08	Wide beam, depression at 0°	6.6 at ±31°	4.7	3.57:1
0.09	Wide beam, depression at 0°with more ripple	6.16 at ±29°	3.15	3.69:1
0.1	Wide beam, depression at 0°with more ripple	6.27 at ±31°	1.98	3.53:1
0.11	Wide beam, depression at 0°with more ripple	6.16 at ±29°	1.66	3.33:1
0.12	Wide beam, depression at 0°with ripple	5.92 at ±30°	0.58	3.9:1
0.13	Wide beam, depression at 0°with ripple	6.42 at±29°	-1.27	3.41:1
0.14	Wide beam, depression at 0°with ripple	6.52 at ±30°	-1.82	3:1
0.15	Wide beam, depression at 0°with ripple	6.52 at ±30°	-2.54	4.08:1
0.16	Wide beam, depression at 0°with ripple	6.7 at ±31°	-4.6	3.08:1
0.18	Wide beam, depression at 0°, large amount of ripple	6.85 at ±30°	-1.3	4.47:1
0.2	Very rippled, distorted beam	6.6	-	3.92:1
0.22	Very rippled, distorted beam	7.2	-	2.3:1
0.24	Very rippled, distorted beam	6.7	-	1.73:1
0.26	Very rippled, distorted beam	6.2	-	2.95:1
0.28	Very rippled, distorted beam	5.8	-	6.34:1
0.3	Very rippled, distorted beam	6.3	-	6.55:1

D.1.4.5 P= 0.5 λ

For P = 0.5λ wide beams with some side ripple were found between R=0.02λ and R=0.06λ. All other patterns displayed a large amount of ripple. VSWR was below 4.5:1 for all antennas. All results can be seen in Table D.29.

Table D.29: Results for N=5, P=0.5 λ

Radius(λ)	**Shape of Pattern and Comments**	**Maximum Gain(dB)**	**Gain at centre if applicable(dB)**	**VSWR**
0.02	Wide beam, 41°HPBW	8.5	-	8.17:1
0.04	Wide beam with depression at 0°	7.05 at 36°	3.41	1.96:1
0.05	Wide beam with depression at 0°	6.87 at 46°	1.22	3.32:1
0.06	Wide beam with depression at 0°	6.44 at 47°	0.49	3.69:1
0.07	Wide beam with depression at 0°, more ripple	5.66 at 46°	0.79	3.17:1
0.08	Wide beam with depression at 0°, more ripple	5.36 at 45°	1.01	3.54:1
0.1	Wide beam with depression at 0°, more ripple	5.1	-0.97	3.62:1
0.12	Wide beam with depression at 0°, more ripple	4.8	-0.92	3.56:1
0.14	Wide beam with depression at 0°, more ripple	5.54	-4.7	3.3:1
0.16	Wide beam with depression at 0°, more ripple	6.08	-6.8	4.09:1
0.18	Wide beam with depression at 0°, more ripple	6.8	-9.7	3.12:1
0.2	Wide beam, very rippled	6.5	-	2.27:1
0.22	Wide beam, very rippled	5.9	-	3.99:1
0.24	Wide rippled beam	7.5	-	5.6:1
0.26	Wide beam,depression at centre, ripple in side lobes	6.43 at 27°	2.86	5.73:1
0.28	Wide beam, very rippled	5.8	-	4.36:1
0.3	Wide beam, very rippled	5.9	-	1.73:1

D.1.4.6 P= 0.6 λ

For P = 0.6λ wide beams (with slight bump at 0°) were noted for R=0.01λ to 0.03λ. All other patterns were very rippled. All VSWRs were below 5:1 for R>0.03λ. All results can be seen in Table D.30.

Table D.30: Results for N=5, P=0.6 λ

Radius(λ)	**Shape of Pattern and Comments**	**Maximum Gain(dB)**	**Gain at centre if applicable(dB)**	**VSWR**
0.01	Wide beam, decreasing to 0°, slight increase at 0°	8.29 at 50°	-11.1	7.45:1
0.02	Wide beam, decreasing to 0°, slight increase at 0°	8.15 at 52°	-5.2	5.68:1
0.03	Wide beam, lower in middle, depressions at 30°	7.57 at 56°	-3.03	5.06:1
0.04	Wide beam, depressions at 32°	7.44 at 57°	-2.93	2.86:1
0.05	Wide,rippled beam, depressions at 32°	6.77 at 59°	-3.69	2.52:1
0.06	Wide rippled beam	6.4	-	3.54:1
0.08	Wide,rippled beam	5.6	-	3.32:1
0.1	Wide,rippled beam	5.5	-	3.71:1
0.12	Wide,rippled beam	5.2	-	3.47:1
0.13	Wide, rippled beam	5	-	3.72:1
0.14	Wide,rippled beam	5	-	3.79:1
0.16	Wide,rippled beam	6.1	-	3.5:1
0.18	Wide,rippled beam	6.7	-	2.94:1
0.2	Wide,rippled beam	6.6	-	4.32:1
0.22	Wide,rippled beam	6.1	-	4.17:1
0.24	Wide,rippled beam	7.1	-	2.48:1
0.26	Wide,rippled beam	6.6	-	1.66:1
0.28	Wide,rippled beam	6.3	-	2.0:1
0.3	Wide,rippled beam	6.3	-	4.73:1

D.1.4.7 P= 0.7 λ

All radiation patterns for P=0.7λ were either distorted or very rippled. VSWR was generally below 5:1. All results can be seen in Table D.31.

Table D.31: Results for N=5, P=0.7 λ

Radius(λ)	**Shape of Pattern and Comments**	**Maximum Gain(dB)**	**Gain at centre if applicable(dB)**	**VSWR**
0.01	Multiple lobes	8.9	-	7.89:1
0.02	Multiple lobes	8.6	-	5.42:1
0.03	Wide beam with lots of ripple	8.4	-	5.43:1
0.04	Wide, rippled beam	8	-	3.74:1
0.06	Wide, rippled beam	7.1	-	3.09:1
0.08	Wide,rippled beam	6.0	-	3.43:1
0.1	Wide,rippled beam	6.3	-	3.72:1
0.12	Wide,rippled beam	6.3	-	3.51:1
0.14	Wide,rippled beam	6.2	-	3.82:1
0.16	Wide,rippled beam	6.2	-	3.25:1
0.18	Wide,rippled beam. Large depression at 0°	6.15	-	3.9:1
0.2	Wide,rippled beam. Large depression at 0°	7.1	-	3.67:1
0.22	Wide,rippled beam. Large depression at 0°	6.5	-	3.82:1
0.24	Wide,rippled beam. Large depression at 0°	6.4	-	3.82:1
0.26	Multiple, rippled lobes	7.7	-	5.28:1
0.28	Wide rippled beam	6.8	-	5.46:1
0.3	Multiple, rippled lobes	6.4	-	4.46:1

D.1.4.8 P= 0.8 λ

All radiation patterns for P=0.8λ were very rippled. VSWR was generally below 4:1. All results can be seen in Table D.32.

Table D.32: Results for N=5, P=0.8 λ

Radius(λ)	**Shape of Pattern and Comments**	**Maximum Gain(dB)**	**Gain at centre if applicable(dB)**	**VSWR**
0.02	Wide, rippled beam	9.2	-	5.38:1
0.04	Wide, rippled beam	8.6	-	4.46:1
0.06	Wide, rippled beam	7.8	-	2.72:1
0.08	Wide, rippled beam	7.8	-	3.66:1
0.1	Wide, rippled beam	8.3	-	3.6:1
0.12	Wide, rippled beam	7.8	-	3.63:1
0.14	Wide, rippled beam	7.4	-	3.7:1
0.16	Wide, rippled beam	6.8	-	3.53:1
0.18	Wide, rippled beam	6.4	-	3.9:1
0.2	Wide, rippled beam	7.1	-	2.93:1
0.22	Wide, rippled beam	6.5	-	3.82:1
0.24	Wide, rippled beam	5.8	-	4.67:1
0.26	Wide, rippled beam. Multiple lobes	7.7	-	3.34:1
0.28	Wide, rippled beam. Multiple lobes	6.8	-	2.38:1
0.3	Wide, rippled beam. Multiple lobes	6.7	-	3.1:1

D.1.5 Results for N = 6 Turns

D.1.5.1 Pitch= 0.1 λ

For P=0.1λ smooth radiation patterns suitable for general use were found for R=0.04λ to R=0.3λ. VSWR performance was very poor for R=0.04λ to R=0.1λ and for R=0.22λ to R=0.3λ. All results can be seen in Table D.33.

Table D.33: Results for N=6, P=0.1 λ

Radius(λ)	**Shape of Pattern and Comments**	**Maximum Gain(dB)**	**Gain at centre if applicable(dB)**	**VSWR**
0.04	Smooth beam	-5.3	-	81.6:1
0.06	Smooth beam, depressions at $\pm$43°	-4.6	-	96.5:1
0.08	Smooth beam, depressions at $\pm$38°	4.3	-	15.4:1
0.1	Smooth beam, depressions at $\pm$32°	7.4	-	31:1
0.12	Smooth beam, 28°HPBW. Slight side lobes	10.9	-	4.53:1
0.14	Smooth beam, 31°HPBW. Slight side lobes	10.3	-	1.99:1
0.16	Smooth beam, 28°HPBW. Slight side lobes	10.4	-	2.19:1
0.18	Smooth beam, 31°HPBW. Slight side lobes	10.6	-	2.06:1
0.2	Smooth beam, 38°HPBW.	8.2	-	5.3:1
0.22	Smooth beam, 37°HPBW.	9.2	-	11:1
0.24	Smooth beam, 32°HPBW.	9.2	-	21.9:1
0.26	Smooth beam, 31°HPBW.	8.8	-	13.9:1
0.28	Smooth beam, 40°HPBW.	6.8	-	44.8:1
0.3	Smooth beam, 53°HPBW.	7.4	-	10.2:1

D.1.5.2 Pitch= 0.2 λ

For P=0.2λ acceptable patterns were found at R=0.02λ,0.06λ and 0.08λ. Patterns with ripple at the side were found for R=0.1λ to R=0.22λ. For R$>$0.22λ large amount of ripple was present. VSWR performance was unacceptably high for R$<$0.1λ. All results can be seen in Table D.34.

Table D.34: Results for N=6, P=0.2 λ

Radius(λ)	**Shape of Pattern and Comments**	**Maximum Gain(dB)**	**Gain at centre if applicable(dB)**	**VSWR**
0.02	Smooth beam, 45°HPBW	-0.53	-	96.8:1
0.04	Multiple lobes	-1.0	-	30.9:1
0.06	Smooth beam, depression at 0°	7.14 at $\pm$27°	5.7	53.5:1
0.08	Smooth beam, 35°HPBW	8.3	-	32.9:1
0.1	Wide beam, slightly distorted. 30°HPBW	9.8	-	2.89:1
0.12	Wide beam, slightly distorted. 27°HPBW	8.9	-	2.46:1
0.14	Wide beam, slightly distorted. 30°HPBW	8.9	-	2.52:1
0.16	Wide beam, slightly distorted/rippled. 28°HPBW	9.1	-	3.14:1
0.2	Slight depression at 0°. Ripple present at side of pattern	7.08 at $\pm$20°	5.56	4.19:1
0.22	Rippled beam	7.1	-	1.33:1
0.24	Rippled beam	6.1	-	8.06:1
0.26	Rippled beam with sidelobes present	7.1	-	1.76:1
0.28	Rippled beam	7.4	-	12:1
0.3	Rippled beam	6.7	-	1.61:1

D.1.5.3 Pitch= 0.3 λ

For P=0.3λ patterns with ripple at the side were found for R=0.06λ to R=0.1λ. All other patterns either had a large amount of ripple, high side lobes or were distorted.VSWR performance was unacceptably high for R$<$0.08λ. All results can be seen in Table D.35.

Table D.35: Results for N=6, P=0.3 λ

Radius(λ)	**Shape of Pattern and Comments**	**Maximum Gain(dB)**	**Gain at centre if applicable(dB)**	**VSWR**
0.04	Multiple lobes	9	-	19.5:1
0.06	Multiple lobes	10.3	-	24.2:1
0.08	Single lobe,31°HPBW.Ripple present at side of lobe	8.9	-	3.95:1
0.1	Single lobe,31°HPBW.Ripple present at side of lobe	7.47	-	3.22:1
0.12	Single lobe,28°HPBW.Ripple present at side of lobe	7.3	-	3.24:1
0.14	Single lobe,28°HPBW.Ripple present at side of lobe	6.83	-	3.75:1
0.16	Single lobe,28°HPBW.Ripple present at side of lobe	7.5	-	4.27:1
0.18	Ripple present at side of lobe	7.6	-	4.46:1
0.2	Ripple present at side of lobe	7		4.72:1
0.22	Rippled beam	6.6	-	5.72:1
0.24	Rippled beam	7.1	-	4.04:1
0.26	Rippled beam	6.2	-	3.47:1
0.28	Rippled beam	5.8	-	5.22:1
0.3	Rippled beam	5.3	-	4.4:1

D.1.5.4 Pitch= 0.4 λ

For P=0.4λ patterns with ripple at the side were found for R=0.06λ to R=0.12λ. All other patterns either had a large amount of ripple, high side lobes or multiple lobes.VSWR performance was generally below 5:1. All results can be seen in Table D.36.

Table D.36: Results for N=6, P=0.4 λ

Radius(λ)	**Shape of Pattern and Comments**	**Maximum Gain(dB)**	**Gain at centre if applicable(dB)**	**VSWR**
0.04	Smooth lobe with side lobes. 25°HPBW	12.7	-	4.29:1
0.06	Single lobe with ripple at side	8.3 at $\pm$40°	7.5	3.08:1
0.08	Rippled beam	6.3	-	3.51:1
0.1	Rippled beam	6.1	-	3.36:1
0.12	Rippled beam	6.2	-	3.63:1
0.14	Rippled beam	6.3	-	3.97:1
0.16	Rippled beam	7.0	-	3.61:1
0.18	Rippled beam	7.4	-	2.72:1
0.2	Rippled beam, Extreme depression at 0°	6.8	-	1.94:1
0.22	Rippled beam	6.9	-	1.66:1
0.26	Rippled beam	5.8	-	6.46:1
0.3	Rippled beam	5.6	-	7.64:1

D.1.5.5 Pitch= 0.5 λ

For P=0.5λ acceptable patterns were found for R=0.02λ to R=0.05λ. The radiation patterns at R=0.04λ and R=0.05λ displayed a depression at 0°. All other patterns were either very rippled or distorted. VSWR was generally below 5:1. All results can be seen in Table D.37.

Table D.37: Results for N=6, P=0.5 λ

Radius(λ)	**Shape of Pattern and Comments**	**Maximum Gain(dB)**	**Gain at centre if applicable(dB)**	**VSWR**
0.02	Smooth beam 40°HPBW	9.5	-	6.7:1
0.04	Smooth beam, depression at 0°	7.62 at ±40°	2.34	2.53:1
0.05	Smooth beam, depression at 0°	7.3 at ±43°	0.88	3.61:1
0.06	Rippled beam	6.3	-	3.1:1
0.08	Rippled beam	5.5	-	3.57:1
0.1	Rippled beam	5.6	-	3.47:1
0.12	Rippled beam	5.2	-	3.74:1
0.14	Rippled beam	5.8	-	3.78:1
0.16	Rippled beam	6.8	-	3.07:1
0.18	Very rippled beam	7.0	-	2.55:1
0.2	Very rippled beam	6.2	-	2.91:1
0.22	Very rippled beam	6.9	-	3.58:1
0.24	Very rippled beam	7.0	-	3.2:1
0.26	Rippled beam	6.5	-	1.27:1
0.28	Rippled beam, Multiple lobes	6.0	-	5.02:1
0.3	Rippled beam. Multiple lobes	5.7	-	2.88:1

D.1.5.6 Pitch= 0.6 λ

For P=0.6λ there were no useful radiation patterns found. All radiation patterns were very rippled. VSWR performance was generally lower than 5:1. All results are shown in Table D.38.

Table D.38: Results for N=6, P=0.6 λ

Radius(λ)	**Shape of Pattern and Comments**	**Maximum Gain(dB)**	**Gain at centre if applicable(dB)**	**VSWR**
0.02	Distorted beam	8.8	-	5.29:1
0.04	Rippled beam	7.7	-	2.48:1
0.06	Rippled beam	6.6	-	3.17:1
0.08	Rippled beam	5.9	-	3.59:1
0.1	Rippled beam	5.7	-	3.53:1
0.12	Rippled beam	5.1	-	3.53:1
0.14	Rippled beam	5.49	-	3.66:1
0.16	Rippled beam	6.4	-	3.1:1
0.18	Rippled beam	6.1	-	3.31:1
0.2	Rippled beam	7.1	-	4.23:1
0.22	Rippled beam	9.0	-	4.96:1
0.24	Rippled beam	8.5	-	5.45:1
0.26	Rippled beam	6.9	-	5.79:1
0.28	Rippled beam	7.4	-	3.2:1
0.3	Rippled beam	6.5	-	3.03:1

D.1.5.7 Pitch= 0.7 λ

For P=0.7λ there were no useful radiation patterns found. All radiation patterns were very rippled or had multiple lobes. VSWR was generally lower than 4:1. All results are shown in Table D.39.

Table D.39: Results for N=6, P=0.7 λ

Radius(λ)	**Shape of Pattern and Comments**	**Maximum Gain(dB)**	**Gain at centre if applicable(dB)**	**VSWR**
0.02	Very rippled beam	9.3	-	4.02:1
0.04	Very rippled beam	8.4	-	2.83:1
0.06	Rippled beam	7.2	-	3.15:1
0.08	Rippled beam	6.5	-	3.59:1
0.1	Rippled beam	6.3	-	3.55:1
0.12	Rippled beam	6.4	-	3.71:1
0.14	Rippled beam	6.2	-	3.29:1
0.16	Rippled beam	6.2	-	3.29:1
0.18	Rippled beam	7.3	-	3.78:1
0.2	Rippled beam	8.5	-	4.26:1
0.22	Rippled beam	9.5	-	3.83:1
0.24	Very rippled beam	8.5	-	3.18:1
0.26	Rippled beam	7.0	-	3.41:1
0.28	Rippled beam	6.6	-	5.83:1
0.3	Multiple lobes	6.6	-	4.93:1

D.1.5.8 Pitch= 0.8 λ

No useful radiation patterns found for P=0.7λ. All radiation patterns were very rippled. VSWR was generally lower than 5:1. All results are shown in Table D.40.

Table D.40: Results for N=6, P=0.8 λ

Radius(λ)	**Shape of Pattern and Comments**	**Maximum Gain(dB)**	**Gain at centre if applicable(dB)**	**VSWR**
0.02	Rippled beam	9.8	-	2.13:1
0.04	Rippled beam	9.1	-	3.64:1
0.06	Rippled beam	8.1	-	3.01:1
0.08	Rippled beam	8.0	-	3.6:1
0.1	Rippled beam	8.5	-	3.57:1
0.12	Rippled beam	7.9	-	3.68:1
0.14	Rippled beam	7.6	-	3.67:1
0.16	Rippled beam	7.0	-	3.44:1
0.18	Rippled beam	7.0	-	3.91:1
0.2	Rippled beam	7.8	-	3.85:1
0.22	Rippled beam	8.7	-	2.91:1
0.24	Rippled beam	7.7	-	2.21:1
0.26	Rippled beam	7.2	-	1.91:1
0.28	Rippled beam	6.4	-	1.75:1
0.3	Rippled beam	7.3	-	5.48:1

D.1.6 Results for N = 7 Turns

D.1.6.1 Pitch = 0.1λ

For P = 0.1λ smooth beams were found for R = 0.24λ to R= 0.3λ. All other radiation patterns showed multiple beams or a large amount of ripple. VSWR performance was generally poor with the exception of R = 0.14λ to 0.18λ. All results can be seen in Table D.41.

Table D.41: Results for N=7, P=0.1 λ

Radius(λ)	**Shape of Pattern and Comments**	**Maximum Gain(dB)**	**Gain at centre if applicable(dB)**	**VSWR**
0.06	Wide beam with deep depressions at $\pm$56°	1.5	-	577:1
0.08	Small vertical lobe, wide sidelobes	-4	-	19.9:1
0.1	Small vertical lobe, wide sidelobes	-1.5	-	25.1:1
0.12	Smooth lobe, 26°HPBW. Side lobes present	9.4	-	33.1:1
0.14	Smooth lobe, 34°HPBW. Side lobes present	9.7	-	1.61:1
0.16	Smooth lobe, 36°HPBW. Side lobes present	9.6	-	1.79:1
0.18	Smooth lobe, 40°HPBW. Side lobes present	8.6	-	4.47:1
0.2	Smooth lobe, 37°HPBW. Side lobes present	8.4	-	9.46:1
0.22	Smooth lobe, 39°HPBW. Side lobes present	7.9	-	20.9:1
0.24	Smooth lobe, 40°HPBW	7.1	-	22.1:1
0.26	Smooth lobe, 47°HPBW	6.5	-	5.62:1
0.28	Smooth beam, 51°HPBW	6.8	-	9.49:1
0.3	Smooth beam, 56°HPBW	6.6	-	47.3:1

D.1.6.2 Pitch = 0.2λ

For P = 0.2λ all patterns showed ripple at the side of the beam. For R=0.1λ to R=14λ the pattern was smooth(at the top) with a depression at 0 $^{\circ}$at all in this range except R =0.1λ. For R$>$0.16 all patterns showed a large amount of ripple. VSWR was varied with the best at R=0.16λ and R=0.18λ and the worst at 0.24λ. All results can be seen in Table D.42.

Table D.42: Results for N=7, P=0.2 λ

Radius(λ)	**Shape of Pattern and Comments**	**Maximum Gain(dB)**	**Gain at centre if applicable(dB)**	**VSWR**
0.06	Multiple lobes	7.5	-	13.1:1
0.08	Multiple lobes	9.8	-	26.8:1
0.1	Wide beam. 39°HPBW. Ripple at side of beam	8.4	-	3.57:1
0.12	Wide beam. Depression at 0°. Ripple at side of beam	7.47 at $\pm$30°	5.37	2.44:1
0.14	Wide beam. Depression at 0°. Ripple at side of beam	7.58 at $\pm$29°	3.08	2.05:1
0.16	Wide beam. Depression at 0°. Ripple at side of beam	7.7 at $\pm$30°	0.41	1.64:1
0.18	Depression at 0°.Large amount of ripple at side of beam	7.3 at $\pm$30°	0.71	1.56:1
0.2	Rippled beam	6.6	-	3.94:1
0.22	Flat beam. Depression at 0°	7.3 at $\pm$31°	3.87	4.44:1
0.24	41°HPBW. Ripple at side of beam	7.1	-	8.15:1
0.26	39°HPBW. Ripple at side of beam	6.9	-	5.98:1
0.28	36°HPBW. Ripple at side of beam	7.2	-	1.87:1
0.3	Smooth beam, significant side lobes	7.0	-	5.19:1

D.1.6.3 Pitch = 0.3λ

For P = 0.3λ the only acceptable radiation patterns were for R=0.06λ to R=0.1λ and these patterns contained ripple in the side of the pattern. All other patterns displayed multiple lobes (for R $<$ 0.06λ) or a large amount of ripple (for R $>$ 0.08λ). VSWR was generally below 4:1 with exceptions at R = 0.02λ,0.03λ, 0.04λ, 0.22λ, 0.26λ. All results can be seen in Table D.43.

Table D.43: Results for N=7, P=0.3 λ

Radius(λ)	**Shape of Pattern and Comments**	**Maximum Gain(dB)**	**Gain at centre if applicable(dB)**	**VSWR**
0.02	Multiple lobes	9.4	-	225:1
0.04	Multiple lobes	6.6	-	80.4:1
0.06	Flat lobe at top. Depression at 0°. Side lobes present	7.68 at $\pm$32°	4.16	16:1
0.08	Smooth at top. 28°HPBW. Ripple at side of beam	9.2	-	3.4:1
0.1	Rippled beam	7.1	-	3.18:1
0.12	Rippled beam	7.1	-	2.98:1
0.14	Rippled beam	7.1	-	2.98:1
0.16	Very rippled beam	7.3	-	2.48:1
0.18	Very rippled beam	8.9	-	1.98:1
0.2	Rippled beam	9.2	-	1.4:1
0.22	Rippled beam	7.9	-	20.9:1
0.24	Rippled beam	8.0	-	3.35:1
0.26	Rippled beam	7.4	-	7.11:1
0.28	Rippled beam	6.3	-	4.82:1
0.3	Rippled beam	5.9	-	1.86:1

D.1.6.4 Pitch = 0.4λ

For P=0.4λ all patterns displayed a large amount of ripple. VSWR performance was below 4:1 for $0.06\lambda < R < 0.28\lambda$. All results can be seen in Table D.44.

Table D.44: Results for N=7, P=0.4 λ

Radius(λ)	**Shape of Pattern and Comments**	**Maximum Gain(dB)**	**Gain at centre if applicable(dB)**	**VSWR**
0.02	Multiple lobes	17.6	-	448:1
0.04	Narrow beam, 22°HPBW. Ripple present at side of lobe	13.4	-	4.94:1
0.06	41°HPBW. Ripple present at side of lobe	8.5	-	3.52:1
0.08	Rippled beam	6.7	-	3.63:1
0.1	Rippled beam	6.3	-	3.43:1
0.12	Rippled beam	6.4	-	3.22:1
0.14	Rippled beam	7.0	-	3.14:1
0.16	Rippled beam	7.6	-	3.15:1
0.18	Rippled beam	7.8	-	3.1:1
0.2	Rippled beam	7.0	-	2.6:1
0.22	Rippled beam	7.0	-	1.42:1
0.24	Rippled beam	6.7	-	4.69:1
0.26	Rippled beam	6.7	-	2.24:1
0.28	Rippled beam	5.7	-	6.56:1
0.3	Rippled beam	5.6	-	5.13:1

D.1.6.5 Pitch = 0.5λ

For P = 0.5λ all patterns with the exception of R=0.02λ showed an unacceptable amount of ripple. VSWR performance was below 5:1 for all antennas. All results can be seen in Table D.45.

Table D.45: Results for N=7, P=0.5 λ

Radius(λ)	**Shape of Pattern and Comments**	**Maximum Gain(dB)**	**Gain at centre if applicable(dB)**	**VSWR**
0.02	Depression at 0°but ripple at side of lobe	9.7 at $\pm$27°	8.2	5.22:1
0.04	Depression at 0°but ripple at side of lobe	8.2 at $\pm$39°	1.7	3.26:1
0.05	Depression at 0°but ripple at side of lobe	7.12 at $\pm$39°	1.13	3.13:1
0.06	Rippled beam	6.8	-	3.26:1
0.08	Rippled beam	5.6	-	3.56:1
0.1	Rippled beam	5.2	-	3.61:1
0.12	Rippled beam	5.6	-	3.38:1
0.14	Rippled beam	6.3	-	3.28:1
0.16	Rippled beam	6.8	-	3.4:1
0.18	Rippled beam	6.8	-	3.65:1
0.2	Rippled beam	5.9	-	3.8:1
0.22	Rippled beam	7.7	-	3.16:1
0.24	Rippled beam	6.1	-	1.48:1
0.26	Rippled beam	5.8	-	5.58:1
0.28	Rippled beam	6.5	-	1.14:1
0.3	Rippled beam	6.4	-	4.9:1

D.1.6.6 Pitch = 0.6λ

For P = 0.6λ all patterns showed an unacceptable amount of ripple. VSWR was below 4:1 for all antennas. All results can be seen in Table D.46.

Table D.46: Results for N=7, P=0.6 λ

Radius(λ)	**Shape of Pattern and Comments**	**Maximum Gain(dB)**	**Gain at centre if applicable(dB)**	**VSWR**
0.02	Large side lobes	9.3	-	2.04:1
0.04	Rippled beam	8.3	-	3.48:1
0.06	Rippled beam	6.8	-	3.3:1
0.08	Rippled beam	5.8	-	3.45:1
0.1	Rippled beam	5.3	-	3.67:1
0.12	Rippled beam	5.3	-	3.56:1
0.14	Rippled beam	5.3	-	3.35:1
0.16	Rippled beam	6.7	-	3.42:1
0.18	Rippled beam	8.2	-	3.74:1
0.2	Rippled beam	9.2	-	4.13:1
0.22	Rippled beam	8.7	-	4.33:1
0.24	Rippled beam	6.4	-	3.29:1
0.26	Rippled beam	5.8	-	1.76:1
0.28	Rippled beam	6.0	-	6.46:1
0.3	Rippled beam	6.9	-	2.64:1

D.1.6.7 Pitch = 0.7λ

For P = 0.7λ all patterns were very rippled. VSWR ranged from 2:1 to 4.5:1. Results can be seen in Table D.47.

Table D.47: Results for N=7, P=0.7 λ

Radius(λ)	**Shape of Pattern and Comments**	**Maximum Gain(dB)**	**Gain at centre if applicable(dB)**	**VSWR**
0.04	Rippled beam	8.8	-	2.96:1
0.06	Rippled beam	7.4	-	3.41:1
0.08	Rippled beam	6.6	-	3.47:1
0.1	Rippled beam	6.1	-	3.6:1
0.12	Rippled beam	6.3	-	3.71:1
0.14	Rippled beam	6.3	-	3.47:1
0.16	Rippled beam	6.4	-	3.71:1
0.18	Rippled beam	7.0	-	3.47:1
0.2	Rippled beam	7.4	-	4.07:1
0.22	Rippled beam	6.8	-	4.52:1
0.25	Rippled beam	7.7	-	3.32:1
0.26	Rippled beam	5.9	-	2.73:1
0.28	Rippled beam	6.1	-	3.31:1
0.3	Rippled beam	7.4	-	4.5:1

D.1.6.8 Pitch = 0.8λ

For P = 0.8λ all patterns were very rippled. VSWR ranged from 2:1 to 6.53:1. Results can be seen in Table D.48.

Table D.48: Results for N=7, P=0.8 λ

Radius(λ)	**Shape of Pattern and Comments**	**Maximum Gain(dB)**	**Gain at centre if applicable(dB)**	**VSWR**
0.02	Rippled beam	10.4	-	5.72:1
0.04	Rippled beam	9.5	-	2.13:1
0.06	Rippled beam	8.2	-	3.37:1
0.08	Rippled beam	8.1	-	3.34:1
0.1	Rippled beam	8.4	-	3.56:1
0.12	Rippled beam	8.0	-	3.72:1
0.14	Rippled beam	7.5	-	3.66:1
0.16	Rippled beam	6.9	-	3.4:1
0.18	Rippled beam	6.3	-	3.49:1
0.2	Rippled beam	6.0	-	3.9:1
0.22	Rippled beam	8.5	-	4.38:1
0.24	Rippled beam	10.0	-	4.81:1
0.26	Rippled beam	6.8	-	4.29:1
0.28	Rippled beam	6.7	-	1.7:1
0.3	Rippled beam	7.2	-	6.53:1

D.1.7 Results for N = 8 Turns

D.1.7.1 Pitch = 0.1λ

For R = 0.1λ patterns with a central depression were found for R = 0.04λ to 0.08λ and 0.14λ to 0.18λ. All other patterns showed acceptable, undistorted behaviour. VSWR performance was poor for all except between R = 0.14λ an R=0.16λ. All results can be seen in Table D.49.

Table D.49: Results for N=8, P=0.1 λ

Radius(λ)	**Shape of Pattern and Comments**	**Maximum Gain(dB)**	**Gain at centre if applicable(dB)**	**VSWR**
0.01				
0.04	Depression at 0°	2.37 at ±43°	-0.61	309:1
0.06	Depression at 0°	-2.6 at ±39°	-5	19.6:1
0.08	Depression at 0°	1.79 at ±31°	0.62	15.4:1
0.1	Smooth lobe, 46°HPBW	5.2	-	9.93:1
0.12	Narrow beam 18°HPBW. Rippled sidelobes	11.5	-	20.5:1
0.14	Depression at 0°. Sidelobes present	8.1	-	1.8:1
0.16	Depression at 0°. Sidelobes present	8.06 at ±30°	6.19	2.86:1
0.18	Depression at 0°. Sidelobes present	7.55 ±32°	4.7	8.52:1
0.2	44°HPBW	7.9	-	4.6:1
0.22	44°HPBW	7.8	-	10.9:1
0.24	46°HPBW	7.5	-	22.9:1
0.26	45°HPBW	7.1	-	35.5:1
0.28	47°HPBW	6.7	-	50.5:1

D.1.7.2 Pitch = 0.2λ

For P = 0.2λ all patterns for R $>$ 0.08λ were very rippled. VSWR was below 5:1 for 0.1λ $<$ R $<$ 0.2λ. All results can be seen in Table D.50.

Table D.50: Results for N=8, P=0.2 λ

Radius(λ)	**Shape of Pattern and Comments**	**Maximum Gain(dB)**	**Gain at centre if applicable(dB)**	**VSWR**
0.02	Smooth beam, 31°HPBW	0.9	-	88.2:1
0.06	Bumpy lobe	2.3	-	27.7:1
0.08	20°HPBW. Side lobes present	8.2	-	24.7:1
0.1	Rippled beam	10.1	-	2.92:1
0.12	Rippled beam	8.4	-	2.56:1
0.14	Rippled beam	8.1	-	2.02:1
0.16	Rippled beam	9.0	-	2.86:1
0.18	Rippled beam	9.7	-	4.96:1
0.2	Rippled beam	7.0	-	2.73:1
0.22	Rippled beam	8.6	-	6.69:1
0.24	Rippled beam	8.4	-	8.28:1
0.26	Rippled beam	8.3	-	10.5:1
0.28	Rippled beam	7.9	-	11.9:1
0.3	Rippled beam	6.8	-	11.2:1

D.1.7.3 Pitch = 0.3λ

With the exception of R=0.06λ all radiation patterns for P =0.3λ displayed a large amount of ripple. VSWR was below 5:1 for R$>$ 0.08λ. All results can be seen in Table D.51.

Table D.51: Results for N=8, P=0.3 λ

Radius(λ)	**Shape of Pattern and Comments**	**Maximum Gain(dB)**	**Gain at centre if applicable(dB)**	**VSWR**
0.04	Depression at 0°. Significant ripple at side of pattern	11.9 at $\pm$30°	6.9	386:1
0.06	33°HPBW. Ripple at side of pattern	9.3	-	11.3:1
0.08	33°HPBW. Ripple at side of pattern	8.6	-	3.27:1
0.1	Rippled beam	7.6	-	3.23:1
0.12	Rippled beam	7.3	-	2.92:1
0.14	Rippled beam	7.5	-	2.7:1
0.16	Rippled beam	7.7	-	3.12:1
0.18	Rippled beam	7.4	-	4.55:1
0.2	Rippled beam	6.9	-	4.34:1
0.22	Rippled beam	6.7	-	2.06:1
0.24	Rippled beam	6.8	-	2.65:1
0.26	Rippled beam	6.5	-	3.82:1
0.28	Rippled beam	6.1	-	3.74:1
0.3	Rippled beam	5.9	-	3.11:1

D.1.7.4 Pitch = 0.4λ

For P = 0.4λ no useful radiation patterns were found. All displayed a large amount of ripple. VSWR was below 5:1 for most antennas with R$>$0.04λ. Results can be seen in TableD.52.

Table D.52: Results for N=8, P=0.4 λ

Radius(λ)	**Shape of Pattern and Comments**	**Maximum Gain(dB)**	**Gain at centre if applicable(dB)**	**VSWR**
0.02	Multiple lobes	9.3	-	38.6:1
0.04	20°HPBW	14	-	5.6:1
0.06	39°HPBW, Ripple at side of lobe	8.5	-	3.8:1
0.08	Rippled beam	6.7	-	3.61:1
0.1	Rippled beam	6.4	-	3.56:1
0.12	Rippled beam	6.5	-	3.42:1
0.14	Rippled beam	6.7	-	3.32:1
0.16	Very rippled, distorted beam	8.0	-	3.53:1
0.18	Rippled beam	8.9	-	4.35:1
0.2	Very rippled, distorted beam	8.0	-	4.78:1
0.22	Rippled beam	7.1	-	1.77:1
0.24	Very rippled, distorted beam	7.3	-	5.79:1
0.26	Very rippled, distorted beam	6.4	-	3.28:1
0.28	Very rippled, distorted beam	6.2	-	2.61:1
0.3	Rippled beam	5.9	-	2.28:1

D.1.7.5 Pitch = 0.5λ

For P = 0.5λ no useful radiation patterns were found. All displayed multiple lobes or a large amount of ripple. VSWR was below 4:1 for antennas with R$>$0.02λ. Results can be seen in TableD.53.

Table D.53: Results for N=8, P=0.5 λ

Radius(λ)	**Shape of Pattern and Comments**	**Maximum Gain(dB)**	**Gain at centre if applicable(dB)**	**VSWR**
0.01	Large side lobes present	11.6	-	7.98:1
0.02	Depression at 0°Side lobes present	9.88 at $\pm$27°	7.06	3.88:1
0.03	Depression at 0°Side lobes present	8.84 at $\pm$35°	3.6	1.91:1
0.04	Depression at 0°Side lobes present	8.27 at $\pm$39°	1.56	3.34:1
0.05	Rippled beam	7.2	-	2.95:1
0.06	Rippled beam	6.9	-	3.37:1
0.08	Rippled beam	5.8	-	3.5:1
0.1	Rippled beam	5.5	-	3.68:1
0.12	Rippled beam	5.2	-	3.76:1
0.14	Rippled beam	6.0	-	3.78:1
0.16	Rippled beam	6.8	-	3.9:1
0.18	Rippled beam	7.0	-	4.29:1
0.2	Rippled beam	5.9	-	4.56:1
0.22	Rippled beam	8.0	-	2.76:1
0.24	Rippled beam	7.0	-	3.19:1
0.26	Rippled beam	6.8	-	2.97:1
0.28	Rippled beam	5.9	-	5.7:1
0.3	Rippled beam	6.4	-	7.39:1

D.1.7.6 Pitch = 0.6λ

For the pitch of 0.6λ all radiation patterns were very rippled. VSWR was generally below 5:1. Results can be can be seen in Table D.54.

Table D.54: Results for N=8, P=0.6 λ

Radius(λ)	**Shape of Pattern and Comments**	**Maximum Gain(dB)**	**Gain at centre if applicable(dB)**	**VSWR**
0.02	Rippled beam	9.72	-	1.86:1
0.04	Rippled beam	8.3	-	2.66:1
0.06	Rippled beam	6.8	-	3.28:1
0.08	Rippled beam	5.9	-	3.5:1
0.1	Rippled beam	5.4	-	3.53:1
0.12	Rippled beam	5.2	-	3.62:1
0.14	Rippled beam	5.8	-	3.76:1
0.16	Rippled beam	6.8	-	3.9:1
0.18	Rippled beam	7.8	-	4.05:1
0.2	Rippled beam	8.0	-	4.02:1
0.22	Rippled beam	6.2	-	2.92:1
0.24	Rippled beam	7.7	-	2.16:1
0.26	Rippled beam	7.0	-	5.64:1
0.28	Rippled beam	6.3	-	3.63:1
0.3	Rippled beam	6.9	-	2.28:1

D.1.7.7 Pitch = 0.7λ

The radiation patterns at 0.7λ were all very rippled and not at all useful. VSWR was generally below 5:1. Results can be seen in Table D.55.

Table D.55: Results for N=8, P=0.7 λ

Radius(λ)	**Shape of Pattern and Comments**	**Maximum Gain(dB)**	**Gain at centre if applicable(dB)**	**VSWR**
0.02	Rippled beam	10.4	-	4.04:1
0.04	Rippled beam	9.1	-	2.97:1
0.06	Rippled beam	7.5	-	3.15:1
0.08	Rippled beam	6.2	-	3.46:1
0.1	Rippled beam	5.9	-	3.63:1
0.12	Rippled beam	6.2	-	3.57:1
0.14	Rippled beam	6.2	-	3.49:1
0.16	Rippled beam	6.1	-	3.50:1
0.18	Rippled beam	6.1	-	3.51:1
0.2	Rippled beam	7.7	-	3.33:1
0.22	Rippled beam	9.8	-	2.62:1
0.24	Rippled beam	8.6	-	2.23:1
0.26	Rippled beam	7.5	-	5.45:1
0.28	Rippled beam	7.2	-	1.50:1
0.3	Rippled beam	6.9	-	3.30:1

D.1.7.8 Pitch = 0.8λ

All radiation patterns for Pitch = 0.8λ were very rippled. VSWR was below 6:1 and the results can be seen in Table D.56.

Table D.56: Results for N=8, P=0.8 λ

Radius(λ)	**Shape of Pattern and Comments**	**Maximum Gain(dB)**	**Gain at centre if applicable(dB)**	**VSWR**
0.02	Rippled beam	10.9	-	2.92:1
0.04	Rippled beam	9.7	-	2.88:1
0.06	Rippled beam	8.4	-	3.38:1
0.08	Rippled beam	8.1	-	3.48:1
0.1	Rippled beam	8.6	-	3.59:1
0.12	Rippled beam	8.0	-	3.73:1
0.14	Rippled beam	7.3	-	3.65:1
0.16	Rippled beam	6.8	-	3.44:1
0.18	Rippled beam	7.4	-	3.21:1
0.2	Rippled beam	8.0	-	2.95:1
0.22	Rippled beam	7.6	-	2.58:1
0.24	Rippled beam	7.1	-	2.78:1
0.26	Rippled beam	7.1	-	5.23:1
0.28	Rippled beam	6.8	-	2.25:1
0.3	Rippled beam	6.8	-	5.78:1